Elsevier Editorial System(tm) for Computers in Biology and Medicine

Manuscript Draft

Manuscript Number: CBM-D-19-00348R2

Title: On the Role of Material Properties in Ascending Thoracic Aortic Aneurysms

Article Type: Full Length Article

Keywords: ascending aortic aneurysm; inverse approach, material parameters, aortic aneurysm failure, finite-element analysis

Corresponding Author: Dr. Salvatore Pasta, PhD

Corresponding Author's Institution: Fondazione RiMED

First Author: Federica Cosentino

Order of Authors: Federica Cosentino; valentina agnese; Giuseppe M Raffa; giovanni gentile; diego bellavia; massimiliano zingales; michele pilato; Salvatore Pasta, PhD

Abstract: One of the obstacles standing before the biomechanical analysis of an ascending thoracic aortic aneurysm (ATAA) is the difficulty in obtaining patient-specific material properties. This study aimed to evaluate differences on ATAA-related stress predictions resulting from the elastostatic analysis based on the optimization of arbitrary material properties versus the application of patient-specific material properties determined from ex-vivo biaxial testing. Specifically, the elastostatic analysis relies the on the fact that, if the aortic wall stress does not depend on material properties, the aorta has to be statistically determinate. Finite element analysis (FEA) was applied to a group of nine patients who underwent both angio-CT imaging to reconstruct ATAA anatomies and surgical repair of diseased aorta to collect tissue samples for experimental material testing. Tissue samples cut from excised ATAA rings were tested under equibiaxial loading conditions to obtain experimentally-derived material parameters by fitting stress-strain profiles. FEAs were carried out using both optimized and experimentally-derived material parameters to predict and compare the stress distribution using the mean absolute percentage error (MAPE). Although physiological strains were below yield point (range of 0.08-0.25), elastostatic analysis led to errors on the stress predictions that depended on the type of constitutive model (highest MAPE of 0.7545 for Yeoh model and 0.7683 for Fung model) and ATAA geometry (lowest MAPE of 0.0349 for patient P.7). Elastostatic analysis needs better understanding of its application for determining aneurysm mechanics, and patient-specific material parameters are essential for reliable accurate stress predictions in ATAAs

***Conflict of Interest Statement**

Please wait...

If this message is not eventually replaced by the proper contents of the document, your PDF viewer may not be able to display this type of document.

You can upgrade to the latest version of Adobe Reader for Windows®, Mac, or Linux® by visiting http://www.adobe.com/products/acrobat/readstep2.html.

For more assistance with Adobe Reader visit http://www.adobe.com/support/products/acrreader.html.

Windows is either a registered trademark or a trademark of Microsoft Corporation in the United States and/or other countries. Mac is a trademark of Apple Inc., registered in the United States and other countries. Linux is the registered trademark of Linus Torvalds in the U.S. and other countries.

Reviewer #4

We thank the reviewer for his or her valuable comments. We have taken these comments into careful consideration when preparing the revised manuscript and feel that the critiques led directly to an improved submission. We hope that the reviewer agrees. All changes made to the document were highlighted in yellow.

Specific comments:

Comment 1. Methods described in references (Joldes et al., 2016; Joldes et al., 2017; Lu et al., 2007b; Miller and Lu, 2013) do not assume anywhere statical determinacy. It is the conclusion from the results that if stress demonstrably does not depend on the properties, the structure must be statically determinate. I suggest re-reading these papers.

Reply: We thank the reviewer for the clarification on the meaning of "static determinacy". We therefore rewritten the text to avoid confusion. Please see text in the Abstract that is now:

"Specifically, the elastostatic analysis relies the on the fact that, if the aortic wall stress does not depend on material properties, the aorta has to be statistically determinate."

Please see text in the Introduction that is now

"However, if the stress distribution does not depend on material properties, the structure has to be statically determinate [22,28]. Under this condition, we can eliminate the need for patient-specific material properties and the FEA can be performed with arbitrary material properties because they do not affect the resulting wall stress. Several research groups adopted this approach to compute wall stress of abdominal [22] and ascending aortic aneurysms [23-26]."

Please see also similar corrections in the Discussion and Conclusion

Comment 2. When using linear finite element method, the material does not need to be chosen as very stiff, as the method assumes infinitesimal deformations anyway

Reply: We strictly followed the methodology described by Liu et al 2017 to obtain the "almost-true" stress distribution for the numerical optimization. We adopted very stiff material only to find the "almost-true" stress as described in the paper by Liu and collborators. Nothing was added in the text if it permitted by the reviewer.

Comment 3. AAA is a 3D structure in complex 3D stress state. AAA cannot be reasonably modelled as a thin-walled structure with assumed no transverse stresses. If you computed just one case with proper 3D elements you would see non-negligible variation of stress over the wall thickness. Membrane elements are inappropriate. Justifying the use of membrane elements by stating that other groups committed the same error is unscientific.

Reply: We agree with reviewer comment that AAA is a 3D structure but this paper did not study AAA. This paper was focused on ascending thoracic aortic aneurysms (ATAA). There are many studies suggesting the pathophysiology and mechanics of AAA is different from that of ATAA. Please consider that ATAA do not present thrombus so that thickness is 2 mm and mechanics is mainly governed by in plane-stress. We agree that transverse stress exist but this component is lower than other in plane stress components. Future studies will be performed using brick elements. We agree that AAA can be statically-determinate structure so that we specified that the findings here reported are restricted to the ascending aorta with the following text in the Discussion and Conclusion sections:

“Although the stress analysis of abdominal aortic aneurysms did not depend on material properties [22], the modeling of the ascending aorta as a statically-determinate structure needs further understanding so that the role of material properties is still important for realistic and accurate stress predictions”

“We conclude that the modeling of the ascending aorta as a statically determinate can lead to errors on wall stress predictions in patient-specific FEAs since aortic wall stress was found to depend on the type of constitutive model and ATAA geometry.”

Comment 4.Use of explicit dynamics algorithm with unquantified effects of mass scaling is inappropriate.

Reply: Please consider that mass scaling was applied only at the beginning of the time step. Specifically, mass scaling was performed by scaling the masses of the elements whose element stable time increments was less than the user-supplied time increment of 1.e-7 so that the element stable time increment for these elements becomes equal to the user-supplied time increment. So mass scaling was effective only to few elements (and not to the whole aorta). We investigated the effect on mass scaling that led to a minor change in the results. The following text was added in the methodology to clarify this aspect.

“Mass scaling was performed by scaling the masses of elements whose stable time increments was less than the user-supplied time increment of 1.e-7 s so that the element stable time increment for these elements becomes equal to the user-supplied time increment. This approach has a minor effect on the stress analysis.”

Comment 5. It is a well-known fact that residual stresses in arterial tissues are important. Not including residual stress in the analysis is not a "study limitation" but rather invalidates the results completely. How

to include residual stress is explained e.g. in (Joldes et al., 2018; Polzer et al., 2013). A simple method of incorporating residual stress is available in open source code http://bioparr.mech.uwa.edu.au/

Reply: We agree with the reviewer on the importance of residual stress and will take care of this in future studies. Unfortunately, we did not study AAA and the source code here proposed appears to be focused only to abdominal aneurysms

Comment 6. Table 1 presents the measurement results of diameter and wall thickness. In the absence of information of measurement errors the reliability of this data in difficult to judge.

Reply: Please consider the aortic diameter was measured by experienced radiologists while tissue measurement by a caliper. Radiologists follow a standard protocol for aortic diameter measurements while we agree that the utilization of a caliper is not the best practice for tissue measurements but we have an experience of >100 ATAA sample measurements. The following text was added in the "Study Limitation":

"Caliper-based measurements of tissue thickness can lead to errors which in turn affect aortic wall stress predictions."

Comment 7. Figure given in response to Rev 5 (on p. 8) demonstrates the computational methods used are erroneous. The stress distributions given in the figure violate simple statics (for a given shape of the membrane and given pressure load, one cannot have different tensions…). Also, it is not possible to use Fung or Yeoh models with linear elastic analysis.

I suggest to consider carefully the following references:

(Biehler et al., 2015; Joldes et al., 2016; Joldes et al., 2017; Joldes et al., 2018; Lu et al., 2007a, b; Miller and Lu, 2013; Zelaya et al., 2014)

Reply: Linear elastic analysis using Fung and Yeoh model can be performed in Abaqus and other FEA by considering the effect of geometric nonlinearity as that given by hyperelastic material.

Minor comment:

This reference, given in support of unproven assertion that ""...peak wall stress has been demonstrated to be higher in ruptured compared with non ruptured abdominal aortic aneurysms" is not appropriate.

"A.K. Venkatasubramaniam, M.J. Fagan, T. Mehta, K.J. Mylankal, B. Ray, G. Kuhan, I.C. Chetter, P.T.

McCollum, A comparative study of aortic wall stress using finite element analysis for ruptured and nonruptured abdominal aortic aneurysms, European Journal of Vascular and Endovascular Surgery, 28

(2004) 168-176."

This study did not use patient-specific material properties, patient-specific wall thickness and did not include residual stress. It also use unverified method using shell elements. Therefore, the conclusions about maximum stress values from this paper cannot be used as a justification that higher stress correlates with rupture risk.

Reply: To avoid confusion, the sentence was rewritten as a follow:

“These approaches for risk stratification appeared to be promising since peak wall stress can be calculated from routinely performed CT scans and may be a better predictor of risk of rupture than aortic diameter [13].”

Please consider that this paper not focused on the justification that higher stress correlates with the rupture risk but rather on the role of material properties in FEA of ATAAs.

*Revised manuscript with highlighted changes
Click here to download Revised manuscript with highlighted changes: Inverse Problem_Revised_MARKED.docx
Click here to view linked References

On the Role of Material Properties in Ascending Thoracic Aortic Aneurysms

Federica Cosentino[1,2], Valentina Agnese[3], Giuseppe M Raffa[3], Giovanni Gentile[3], Diego Bellavia[3], Massimiliano Zingales[4], Michele Pilato[3], Salvatore Pasta[2,3*]

[1] Biomedical Department of Internal Medicine and Specialities (DIBIMIS), Piazza delle Cliniche, n.2, 90128, University of Palermo, Palermo, Italy
[2] Fondazione Ri.MED, Via Bandiera n.11, 90133, Palermo, Italy;
[3] Department for the Treatment and Study of Cardiothoracic Diseases and Cardiothoracic Transplantation, IRCCS-ISMETT, Via Tricomi n.5, 90127, Palermo, Italy
[4] Department of Civil, Environmental, Aerospace, Materials Engineering (DICAM), Viale delle Scienze Ed.8, 90128, University of Palermo, Palermo, Italy

Conflict of interest: none

[*] Corresponding author:
Salvatore Pasta, PhD
Professor of Industrial Bioengineering,
Fondazione Ri.MED
Phone: +39 091 3815681
FAX: +39 091 3815682
e-mail: spasta@fondazionerimed.com

Abstract: One of the obstacles standing before the biomechanical analysis of an ascending thoracic aortic aneurysm (ATAA) is the difficulty in obtaining patient-specific material properties. This study aimed to evaluate differences on ATAA-related stress predictions resulting from the elastostatic analysis based on the optimization of arbitrary material properties versus the application of patient-specific material properties determined from *ex-vivo* biaxial testing. Specifically, the elastostatic analysis relies the on the fact that, if the aortic wall stress does not depend on material properties, the aorta has to be statistically determinate. Finite element analysis (FEA) was applied to a group of nine patients who underwent both angio-CT imaging to reconstruct ATAA anatomies and surgical repair of diseased aorta to collect tissue samples for experimental material testing. Tissue samples cut from excised ATAA rings were tested under equibiaxial loading conditions to obtain experimentally-derived material parameters by fitting stress-strain profiles. FEAs were carried out using both optimized and experimentally-derived material parameters to predict and compare the stress distribution using the mean absolute percentage error (MAPE). Although physiological strains were below yield point (range of 0.08-0.25), elastostatic analysis led to errors on the stress predictions that depended on the type of constitutive model (highest MAPE of 0.7545 for Yeoh model and 0.7683 for Fung model) and ATAA geometry (lowest MAPE of 0.0349 for patient P.7). Elastostatic analysis needs better understanding of its application for determining aneurysm mechanics, and patient-specific material parameters are essential for reliable accurate stress predictions in ATAAs.

Keywords: ascending aortic aneurysm; inverse approach, material parameters, aortic aneurysm failure, finite-element analysis

INTRODUCTION

A ruptured ascending thoracic aortic aneurysm (ATAA) is considered a surgical emergency since progressive dilatation is often fatal if this disease is not detected by diagnostic imaging and managed immediately [1]. Despite being a relatively rare event with an estimated incidence of 5.0 per 100,000 individuals per year, the risk of fatal complications such as rupture or acute dissections can be as high as 50% in patients with a large ATAA wall (aortic diameter >50mm) [2, 3]. The risk over time of ATAA development to a size of 40-45mm in patients with a congenital bicuspid aortic valve (BAV) versus the morphological normal tricuspid aortic valve (TAV) is remarkable. Several studies highlighted that 84% of individuals with BAV may develop aortopathy during the life course [4, 5]. With regards to ATAA, degenerative aneurysms tend to develop in the mid-ascending aorta and then progress distally and proximally while ATAAs associated with connective tissue disorders are usually confined to the aortic root [6].

Although the aortic size criterion can be adjusted to achieve higher patient specificity using the body surface area or patient height [7], the surgical dilemma still exists because fatal complications can occur at aortic diameters lower than that dictated by current clinical guidelines for elective repair of aneurysmal aorta [8]. There is a need to delineate additional metrics, not based on aortic size, to better identify the risk of ATAA failure. Biomechanical risk assessments using finite element analysis (FEA) to estimate the wall stress exerted on the diseased aorta have been proposed in abdominal aortic aneurysms [9] [10] and ATAAs [11, 12]. These approaches for risk stratification appeared to be promising since peak wall stress can be calculated from routinely performed CT scans and may be a better predictor of risk of rupture than aortic diameter [13]. Recently, FEA was combined with machine learning techniques to study the relationship between shape features and wall stress as risk metric of ATAA, towards the development of computer-aided-diagnosis [14].

FEAs depend on several factors including the aortic geometry, the loading condition induced by hemodynamic and structural loads and the material properties of aortic wall constituents. Hemodynamic can be evaluated by computational fluid dynamic [15-18] or *in-vivo* 4D flow MRI [19] while tracking algorithms of aortic wall surface detected by dynamic CT [20] or MRI [21] can be adopted to estimate the ATAA-related structural mechanics. Obtaining material parameters non-invasively during patient monitoring for preoperative risk estimations represent an important challenge. However, if the stress distribution does not depend on material properties, the structure has to be statically determinate [22,28]. Under this condition, we can eliminate the need for patient-specific material properties and the FEA can be performed with arbitrary material properties because they do not affect the resulting wall stress. Several research groups adopted this approach to compute wall stress of abdominal [22] and ascending aortic aneurysms [23-26].

In this proof-of-concept, ~~assuming static determinacy for the aorta~~, we want to know how different would be the resulting stress distribution on the aneurysm wall if material properties derived by an elastostatic analysis proposed by Liu et al. [23] are used as compared to FEAs using patient-specific material properties determined from *ex-vivo* biaxial testing. If large differences of stress distributions are observed, one could raise a red flag for further investigation using this appealing approach. To accomplish this task, we carried out FEAs on nine patients who underwent both dynamic CT imaging and surgical elective repair of ATAA to both reconstruct aortic geometries for FEA and collect tissue samples for patient-specific material property evaluation by the fitting of experimental stress-strain curves. Both an isotropic- (ie, two-term Yeoh model) and an anisotropic (ie, Fung-exponential model) constitutive formulation were tested. A stress comparison using the optimal material set versus the experimentally-derived material set was performed, and results were discussed.

METHODS

Study Population

All nine patients included in this investigation had electrocardiogram-gated computed tomography angiography (ECG-gated CT) for the measurement of the maximum aortic diameter and then elective surgical repair of dilated aortas at ISMETT IRCCS hospital institution. ECG-gated CT scans were reconstructed to obtain images at both diastolic and systolic cardiac phases, which were used for the estimation of the diastolic-to-systolic displacement field of the aortic wall. This displacement field was used as a boundary condition for FEA as previously described by our group [27]. Aortic valve shape was classified as TAV versus BAV based on reconstructed images parallel to the aortic valve plane. The presence of the raphe was used to group BAV morphology according to the fusion of right and left cusps (AP) as well as the fusion of right and non-coronary cusp (RL). After surgical ATAA repair, excised aortic tissues were stored in a physiologic solution upon biaxial mechanical testing. Table 1 shows patient demographic information, pre-operative aortic diameters and thickness measurements. The study was approved by the local research ethics committee, and all patients signed informed consent prior enrollment.

Biaxial Testing

Experimentally-related material properties from aneurysmal tissue samples collected for each patient were estimated by equibiaxial mechanical testing using an ElectroForce TestBench system (TA Instrument, Boston, MA). In brief, square specimens (10x10mm) cut form the tissue region located along the major curvature of the aortic ring were extrapolated. Each specimen was oriented along longitudinal and circumferential directions of the aortic vessel while sutures were used to fix specimen edge using surgical staples. Thickness was measured with a caliper for each sample (see Table 1). Five black markers were placed on the intimal aortic tissue surface to evaluate engineering strains along testing directions using a digital video

extensometer placed perpendicular to the testing area. During biaxial loading, the specimen was sub-merged in 0.9% physiologic saline solution in a bath under controlled temperature of 37^{o}C. A small preload (0.5 grams) was set prior to the displacement-driven testing protocol and, after preconditioning, a constant speed of 1mm/min was applied to four electromagnetic motors for loading the specimen under equibiaxial condition. Two 200N load cells were used to record forces along material directions. Data analysis to obtain stress and strain were calculated as defined in the constitutive modeling section.

Constitutive Modeling

FEAs were carried out using two specific classes of materials: a) the isotropic Yeoh material model in the two-term formulation proposed by Raghavan and Vorp [9] for abdominal aortic aneurysms, and b) the orthotropic Fung-exponential model that is often used in soft tissue biomechanics. Both models adopt homogenous, incompressible and hyperplastic description of ATAA wall mechanics.

In short, the two-term Yeoh constitutive model relates the stress tenors (S) in the loaded specimen to the stretch (λ) through the equation:

$$S_{11} = S_{22} = \left[2\, c_1^{(Y)} + 4\, c_2^{(Y)}\, (\lambda^2 + 2\,\lambda^{-1} - 3)\right][\lambda^2 - \lambda^{-1}] \quad (1)$$

with $c_1^{(Y)}$ and $c_2^{(Y)}$ are material model parameters indicative of the mechanical properties of the ATAA wall, and λ is equal to the deformed specimen length divided by the original length. $S_{33} = 0$ according to the membrane stress state assumption adopted in our FEA approach.

The free energy function for the Fung model was:

$$f(\mathbf{C}) = \frac{c_1^{(F)}}{2}\left[\exp\left[Q(\mathbf{C})\right] - 1\right] \quad (2)$$

159 with $\left[c_1^{(F)}\right] = F/L$ the material-like parameter , $\mathbf{C} = \mathbf{F}^T\mathbf{F}$ the right Cauchy-Green strain tensor

160 while the material-dependent exponent, $Q(\boldsymbol{C})$, was a quadratic form of Cauchy-Green strain

161 tensor $\mathbf{C} = \mathbf{F}^T\mathbf{F}$:

162 $$Q(\mathbf{C}) = a_1 I_1^2 + a_2 I_2^2 + 2a_3 I_1 I_2 \quad (3)$$

163 with a_1, a_2, a_3 the dimensionless parameter.

164

165 The Cauchy stresses of Fung constitutive formulation are therefore expressed as:

$$\sigma_{11} = 2\lambda_1^2 c_1^{(F)} e^Q (a_1\lambda_1 + a_3\lambda_2)$$
$$\sigma_{22} = 2\lambda_2^2 c_1^{(F)} e^Q (a_3\lambda_1 + a_2\lambda_2) \quad (4\ a,b)$$

166 ***Constitutive Material Parameter Estimation***

167 The elastostatic analysis for the evaluation of material constitutive parameters proposed by Liu

168 et al [23] is based on the main premise for which the stress distribution is statically determinate.

169 Thus, for a given ATAA deformed configuration (ie, peak of systole) and known loading

170 condition (ie, the diastolic-to-systolic displacement field), different material parameters and

171 constitutive models will give nearly the same stress field. In this way, an “almost-true” stress

172 field at systole can be approximately obtained by an infinitesimal linear elastic model with

173 sufficiently stiff material parameters. This fact has been theoretically justified by Miller and Lu

174 [28] and numerically verified by Lu et al. [29] and Joldes et al. [22]. Given the constitutive model

175 with an initial guess of material parameters (ie, $c_1^{(Y)}$ and $c_2^{(Y)}$ for Yeoh model and $c_1^{(F)}$, a_1, a_2, a_3

176 for the Fung model), by using the constitutive equations and deformation relationship between

177 the two loading states, an optimization algorithm allows to find the “true” material parameters

178 such that the difference between the estimated and “almost-true” stress fields is minimized.

179 Thus, the objective of the optimization process was to find a set of material descriptors that

minimize the difference between the "almost-true" systolic stress, $\tilde{\sigma}^{t}$, and estimated systolic stress, $\tilde{\sigma}^{est}$, for each element as:

$$g_e^{(Y)} = \sum_{m=1}^{N}\sum_{i=1}^{2}\left[\tilde{S}_i^{(t)} - \tilde{S}_i^{(e)}\left(c_1^{(Y)}, c_2^{(Y)}\right)\right]^2$$
$$g_e^{(F)} = \sum_{m=1}^{N}\sum_{i=1}^{2}\left[\tilde{S}_i^{(t)} - \tilde{S}_i^{(F)}\left(c_1^{(F)}, a_1, a_2, a_3\right)\right]^2 \quad \text{(5 a,b)}$$

where N is the number of elements used in each model and i is the component index of each principal stress component. Eq. 1 and Eq. 4 were used for the estimated systolic stress of Yeoh and Fung models, respectively.

The optimization was implemented in the mathematical language program, MATLAB (v2018, Mathworks, MA, USA). Nonlinear least-squares algorithm with trust-region-reflective was used for the optimization of Yeoh material parameters using $c_1^{(Y)} > 0$ and $c_2^{(Y)} > 0$ as lower bounds. For the Fung-exponential form, physically meaningful and plausible material parameters were obtained by enforcing the convexity of the strain energy function and thus performing constrained minimization. For planar biaxial loading of soft tissue, strict convexity physically implies that the projections of the contour of $f(\mathbf{C})$ on the I_1 - I_2 plane form a convex surface [30]. It can be shown that if $c_1^{(F)} > 0$, then Eq. 4 is likely convex if and only if $a_1 > 0$, $a_2 > 0$ and $a_1\, a_2 - a_3^2 > 0$

For the estimation of the "almost-true" systolic stress distribution, we selected a very stiff material for the aortic wall (E=2x10^4 GPa and v=0.49) to obtain Cauchy stress. As initial guess of material descriptors, we used the population-average material properties reported by Pasta et al. [31] for the two-term Yeoh model and by Azdani et al. [32] for the Fung model of ATAAs. For

each optimization procedure, principal stresses were imported in MATALB by postprocessing of ABAQUS models, and the optimization was done to obtain the optimal material parameters.

Computational Study

ECG-gated CT images were used to segment the ATAA wall at both end-diastolic and peak-systolic cardiac phases using the medical imaging software Mimics (Mimics v20, Materialise, Leuven, BE) [15, 33]. Semi-automatic threshold-based segmentation of aortic lumen allowed us to obtain a point cloud (resolution of 0.3 mm), which was triangulated to generate a surface mesh of both diastolic and systolic ATAA geometries. Using an algorithm previously developed by our group in MATLAB (v2018, Mathworks, MA, USA), the point cloud of the diastolic aortic-luminal surface was projected normally onto the systolic aortic-luminal surface to determine the displacement field as the Euclidean distance between closest points [15]. The estimated diastolic-to-systolic displacement field was then implemented as a boundary condition in the FEA model for estimating wall stresses.

For each patient, FEAs were developed using the reconstructed ATAA geometry at diastole, which was meshed with quadrilateral (M3D4R) and triangular (M3D3) membrane elements in ABAQUS/Explicit (v2018, SIMULIA Inc, Providence, RI). Reduced integration was used for the 4-node quadrilateral membrane element. Grid convergence led to an element size of 0.7mm (element range of 28,200-37,500) to obtain a reproducible stress analysis of the human thoracic aorta [34]. Uniform material properties were adopted for the aortic wall while thickness measured from tissue samples was set for each patient simulation. Distal ends of the descending aorta and supra-aortic vessels were fixed in all directions. Material fiber direction was set using multiple cylindrical coordinate systems with origins in the centerline of the aneurysmal aorta. The ATAA wall was modeled using two constitute formulations to assess the

role of the isotropic- and anisotropic material behavior on the resulting stress distribution. The density of the aortic tissue was 1060 kg/m^3. In the Abaqus/Explicit solver, ATAA wall mechanics was modeled as a quasi-static process while the energy was monitored to ensure the ratio of kinetic energy to internal energy remains less than 10%. Adequate time step was applied while an element-by-element stable time increment estimate, coupled with a "variable mass scaling technique," reduced the computational cost of each simulation. Mass scaling was performed by scaling the masses of elements whose stable time increments was less than the user-supplied time increment of 1.e-7 s so that the element stable time increment for these elements becomes equal to the user-supplied time increment. This approach has a minor effect on the stress analysis.

The numerical strategy is here summarized:

1. For the estimation of the "almost-true" stress distribution, the FEA model of each patient was loaded with a uniform peak systolic pressure distribution of 120mmHg in a very stiff aortic wall (E=2x10^4 GPa and v=0.49). This approach led to infinitesimal deformation of aneurysmal aorta.
2. The resulting "almost-true" stress distribution was adopted to optimize the population-average material descriptors of Yeoh and Fung constitutive relationships. This step allowed us to find the optimal material parameters specific to a given patient geometry.
3. A second set of simulations was performed using the optimal material properties and the diastolic-to-systolic displacement field (instead of the uniform pressure distribution) to find realistic deformation of ATAA wall.
4. A third set of simulations was carried out using the displacement field as the boundary condition but using the experimental material properties evaluated from *ex-vivo* material testing. Then, results were compared to those observed for the second set of simulations.

RESULTS

Experimental biaxial testing

Experimental raw data from equibiaxial testing are shown as Piola-Kirchhoff stress versus engineering-strain plots for ATAAs in both circumferential and longitudinal directions of ascending aorta (Figure 1). Most of stress-strain data presented a linear part, related to the elastic properties of the aneurysmal aortic tissue, followed by an exponential part related to the collagen fiber recruitment. These parts were separated by the “yield point”, which is more likely to define the *in-vivo* stress range. For a given tissue specimen, there was no remarkable difference of material response between longitudinal and circumferential directions, suggesting isotropic mechanical behavior for ATAA wall as previously found [31]. Stress-strain data were successfully fit by both the isotropic and anisotropic constitutive models, and the material parameters for each patient were estimated (Table 2). Fitting was able to accurately reproduce the non-linear behavior of experimental data (R^2>0.91 in all cases) so that material descriptors can be considered as determinants of the biomechanical behavior of ATAA wall. After running the elastostatic optimization analysis, material parameters were found close to those obtained from the fitting of the experimental stress-strain curves. We observed that even a variation of 10% on the initial guess of the constitutive parameter set did not determine remarkable changes on the optimal material parameters.

Strain analysis

Figure 2 shows the distribution of diastolic-to-systolic strain field as well as the experimental stress-strain curve from biaxial testing of the aortic tissue specimen cut from the same patient. It can be observed that the range of “true” strain in the circumferential direction is below the yield strain, which is the value of the strain at yield point before reaching the steep increase in the stress-strain response of tested aortic tissue specimen. Most of patients experienced low strain

at CT imaging, except for patients P.6 and P.9 who experience strains remarkably above the yield strain (Table 3). This can be determined by high blood pressure induced by hypertension, increased stretch and twist of aortic vessel due to heart beating and local changes of material properties or tissue thickness, exposing the aneurysmal aorta at greater risk of complications than other patients.

"Almost-true" stress computation

The distribution of "almost-true" stress determined by the simple linear-elastic FEA with the stiff elastic modulus was compared to that obtained at the end of optimization procedure for each patient simulation. Specifically, the maximum principal stress exerted on the ATAA wall was used as an indicator of intramural stress of aneurysmal aorta. Figure 3 shows that the stiff ATAA model had a stress distribution similar to that of Fung model but different from that shown by the Yeoh model. The mean absolute percentage error (MAPE) was calculated for each patient as a measure of differences among simulation approaches. For the patient P.1 shown in Figure 3, the MAPE was nearly 30% between the "almost-true" and Yeoh models and 8.5% between the "almost-true" and Fung models. For other patient cases, we found errors in the range of 6-18%.

Biaxial testing of optimal vs experimental material parameters

Optimized material parameters obtained from elastostatic analysis were used to determine the stress-strain response under equibiaxial loading conditions in a FEA reproducing the experimental testing of aortic tissue sample. Then, the stress-strain curves were plotted together with the experimental testing data (see Figure 4). P.2 with small strain field exhibited a practically equivalent stress-strain response with both experimental and elastostatic material descriptors. At strain of 14%, P.6 had the largest discrepancy of 24% in stress predictions between optimized and experimental material descriptors of two-term Yeoh constitutive model.

Patient-specific FEA of optimal vs experimental material parameters

Figure 5 illustrates predicted wall stress distributions computed by patient-specific material descriptors determined from experimental biaxial testing of Yeoh model. Local maxima of wall stress were mainly placed near the maximum curvature of the ascending aorta, just above the sino-tubular junction. In a similar way, Figure 6 shows predicted wall stress maps resulting from the experimentally-based material fitting using the Fung model. It can be observed that stress distributions are similar among constitutive formulations (ie, Yeoh versus Fung model) when patient-specific material parameters are adopted.

Although biaxial testing results of optimal versus experimental material parameters are encouraging, we found considerable discrepancies for the patient-specific stress predictions between the optimal material parameter set versus the experimentally-derived set (Figure 7). The MAPE was calculated for each patient and evinced highly variable differences from patient to patient and the type of constitutive formulation (see Table 4).

DISCUSSION

In this study, we exploited the appealing concept of obtaining reasonably and accurate stress solutions of aneurysm mechanics using an inverse approach ~~static determinacy~~, and thus without invoking accurate material descriptors that are hard to know before surgical management of ATAAs. ~~Assuming static determinacy for the aorta~~, we optimized population-average material parameters with respect to an “the “almost-true” stress fields obtained with an infinitesimal linear-elastic model based on a sufficiently stiff Young modulus [23]. The so-recovered material parameters were implemented in FEAs, and then stress distributions of nine ATAA geometries were compared to those predicted when patient-specific material descriptors are estimated from the fitting of *ex-vivo* testing data of aortic tissue specimens collected from the same patient. We observed that the stress-strain response under equibiaxial loading

329 predicted by the elastostatic analysis was consistent to the experimental material behavior if
330 strain was low (largest difference of 24% at strain of 14%). This was in agreement with findings
331 documented by Liu et al. [23]. However, the discrepancy on predicted stress distributions was
332 considerably, depending on the adopted constitutive model and ATAA shape, when FEAs were
333 performed on patient anatomies. Although the stress analysis of abdominal aortic aneurysms
334 did not depend on material properties [22], the modeling of the ascending aorta as a statically-
335 determinate structure needs further understanding so that the role of material properties is still
336 important for realistic and accurate stress predictions.
337
338 Identification of patient-specific material parameters of ATAAs deserves important interest as
339 FEAs rely on population-average values of material properties for those patients undergoing
340 close monitoring of the aneurysm size. In risk predictions of aneurysm failure, FEAs based on
341 patient-specific material descriptors were carried out in very few studies restricted to patients
342 who underwent elective surgical repair of ATAA wall to derive the material behavior from
343 uniaxial or bulge inflation tests [11, 12]. The role of material properties in computational growth
344 and remodeling analyses may be even more remarkable as stress estimations are strongly
345 dependents on local material changes [35].
346
347 To avoid *ex-vivo* material testing, inverse approaches allows to estimate material descriptors;
348 however, inverse analysis involves a complex non-linear problem [36, 37]. Most of inverse
349 techniques proposed for soft tissue mechanics attempt to minimize a cost function defined by
350 the difference between a target parameter, which is determined from medical image analysis,
351 and a candidate parameter estimated from FEA and then iteratively adjusted to tune material
352 parameters of interest [38]. However, inverse approaches are commonly time consuming due to
353 continuous interaction with the FEA solver [39]. For the ascending aorta, Trabelsi et al. [38]
354 proposed an inverse method in which the target variable was the volume variation of the aorta

measured from ECG-gated CT scans. They assumed a linear relationship between the constitutive material parameter and the volume of the aortic luminal surface, and then carried out eight FEA analyses for each patient to build datasets for several CT measurements of ATAA volume at systole and mid-cardiac phase. The error attributed to this approach was 0.6% on estimated CT volume and 9.6% on the predicted stress response under equibiaxial test simulations. In agreement with our findings, the statically determinate inverse approach proposed by Liu et al. [23] for the Gasser-Holzapfel-Ogden constitutive model demonstrated comparable biaxial stress-strain curves between elastostatic analyses and experimental tests estimated in a previous investigation of the same group [11]. In their patient study group, patient-specific FEAs on ATAA anatomies were not done because of lack of both CT and tissue data, without quantification of stress changes computed with either experimental or elastostatic-based material parameters.

Generally, the stress of a deformable body depends not only on its geometry, load and boundary conditions, but also on the mechanical properties of constituents. One of the obstacles standing before the biomechanics community is the difficulty in obtaining patient-specific properties of tissues given the absence of a methodology to non-invasively estimate stress *in-vivo*. Notwithstanding, there is an emerging interest from several groups in reformulating computational mechanics in a new paradigm so that computational stress predictions are weakly sensitive to the variation of mechanical properties when the deformed configuration is given [28]. This paradigm can apply to non-linear elastic material, because the stress in such material depends on the relative deformation among two definite configurations. If one of them is known, the other can be solved from equilibrium, which is dominated by in-plane stress for thin-walled structure treated as a membrane. From the analysis of ECG-gated CT images, we observed that strain at deformed configuration bears to the linear-elastic part of the experimental stress-strain response (see Table 3), thereby supporting in part the static

381 determinacy of the aneurysmal wall. In this way, the inverse problem can be directly formulated
382 using the constitutive law as here presented or shown by other studies [23, 40] and without the
383 need of a continuous interaction with the FEA solver. Using the Fung model, Miller et al. [28]
384 investigated the sensitivity of the stress solution with respect to material parameters and
385 constitutive model in three intracranial aneurysm geometries under static determinacy. The
386 inverse stress solution was far less sensitive to material description as, for instance, the 100
387 times increase in the stiffness parameter C of the Fung model led to a 2.9% error in the
388 maximum principal stress prediction. As compared to abdominal or cerebral aneurysms, the
389 ascending aorta is cyclically stretched and twisted every heartbeat by determining the presence
390 of longitudinal and shear stresses in a way that the static equilibrium is not only governed by the
391 internal pressure. These mechanical forces are also highly dynamic (as systole is approximately
392 0.33s), thereby determining viscoelastic effects. These factors combined to residual stress likely
393 occurring in blood vessels can pose several doubts on the modeling of the ascending aorta as
394 statically-determinate structure.
395
396 The major limitation of this study is that comparisons of stress predictions were carried out
397 assuming the experimentally-derived material parameters as the true material descriptors of the
398 ATAA wall, but these can be indeed different from the *in-vivo* condition. However, there is no
399 methodology to *in-vivo* estimate the material behavior so that experimental material parameters
400 are the most accurate ATAA material descriptors. FEAs were based on homogenous thickness
401 and material properties for the whole aorta but there exist evidence of regional changes in the
402 material properties and thickness along the vessel circumference [41] and from the aortic root to
403 the distal ascending aorta [42]. It should be mentioned that the optimization procedure can be
404 modified to account for heterogenous thickness and regionally-dependent material properties by
405 slightly altering the workflow and evaluating the objective function element-by-element.
406 Disregarding the presence of residual stresses and considering the arterial wall as a 3D

membrane with uniform thickness can be considered as additional limitations of the current work. It was assumed that the aortic wall behaves as a membrane with no bending moments or no through thickness shear, although regions near the branches may not satisfy the membrane assumption. The orientation of elastic fiber was not considered in FEAs, and this may alter the stress distribution as demonstrated in a previous study [31]. Caliper-based measurements of tissue thickness can lead to errors which in turn affect aortic wall stress predictions.

CONCLUSION

We conclude that the modeling of the ascending aorta as a statically determinate can lead to errors on wall stress predictions in patient-specific FEAs since aortic wall stress was found to depend on the type of constitutive model and ATAA geometry. Static determinacy needs better understanding of its application to determine ascending aortic aneurysm mechanics so that patient-specific material descriptors as determined by *ex-vivo* material testing are advocated for reliable accurate stress predictions of ATAA wall mechanics.

ACKNOWLEDGMENTS

This work was supported by a “Ricerca Finalizzata” grant from the Italian Ministry of Health (GR-2011-02348129) as well as by a grant from Fondazione RiMED to Salvatore Pasta. Federica Cosentino thanks the Fondazione RiMED and Ministry of Education, University and Research (MIUR) for supporting her PhD programme.

REFERENCES

[1] L.K. Bickerstaff, P.C. Pairolero, L.H. Hollier, L.J. Melton, H.J. Van Peenen, K.J. Cherry, J.W. Joyce, J.T. Lie, Thoracic aortic aneurysms: a population-based study, Surgery, 92 (1982) 1103-1108.

[2] M.A. Coady, J.A. Rizzo, G.L. Hammond, D. Mandapati, U. Darr, G.S. Kopf, J.A. Elefteriades, O.W. Isom, F. Robicsek, R.B. Griepp, What is the appropriate size criterion for resection of thoracic aortic aneurysms?, Journal of Thoracic and Cardiovascular Surgery, 113 (1997) 476-491.

[3] J.A. Beckman, Aortic aneurysms: pathophysiology, epidemiology and prognosis, in: M.A. Creager, V.J. Dzau, J. Loscalzo (Eds.) (eds): Vascular Medicine, Saunders Elsevier, Philadelphia, PA, 2006.

[4] S. Verma, S.C. Siu, Aortic dilatation in patients with bicuspid aortic valve, N Engl J Med, 370 (2014) 1920-1929.

[5] M.A. Borger, P.W.M. Fedak, E.H. Stephens, T.G. Gleason, E. Girdauskas, J.S. Ikonomidis, A. Khoynezhad, S.C. Siu, S. Verma, M.D. Hope, D.E. Cameron, D.F. Hammer, J.S. Coselli, M.R. Moon, T.M. Sundt, A.J. Barker, M. Markl, A. Della Corte, H.I. Michelena, J.A. Elefteriades, The American Association for Thoracic Surgery consensus guidelines on bicuspid aortic valve-related aortopathy: Full online-only version, J Thorac Cardiovasc Surg, 156 (2018) e41-e74.

[6] A. Della Corte, C. Bancone, C. Quarto, G. Dialetto, F.E. Covino, M. Scardone, G. Caianiello, M. Cotrufo, Predictors of ascending aortic dilatation with bicuspid aortic valve: a wide spectrum of disease expression, Eur J Cardiothorac Surg, 31 (2007) 397-404; discussion 404-395.

[7] J.A. Elefteriades, E.A. Farkas, Thoracic aortic aneurysm clinically pertinent controversies and uncertainties, J Am Coll Cardiol, 55 (2010) 841-857.

[8] L.A. Pape, T.T. Tsai, E.M. Isselbacher, J.K. Oh, P.T. O'Gara, A. Evangelista, R. Fattori, G. Meinhardt, S. Trimarchi, E. Bossone, T. Suzuki, J.V. Cooper, J.B. Froehlich, C.A. Nienaber, K.A. Eagle, Aortic diameter >= 5.5 cm is not a good predictor of type A aortic dissection - Observations from the international registry of acute aortic dissection (IRAD), Circulation, 116 (2007) 1120-1127.

[9] M.L. Raghavan, D.A. Vorp, Toward a biomechanical tool to evaluate rupture potential of abdominal aortic aneurysm: identification of a finite strain constitutive model and evaluation of its applicability, Journal of Biomechanics, 33 (2000) 475-482.

[10] M.F. Fillinger, S.P. Marra, M.L. Raghavan, F.E. Kennedy, Prediction of rupture risk in abdominal aortic aneurysm during observation: Wall stress versus diameter, J Vasc Surg, 37 (2003) 724-732.

[11] C. Martin, W. Sun, T. Pham, J. Elefteriades, Predictive biomechanical analysis of ascending aortic aneurysm rupture potential, Acta Biomater, 9 (2013) 9392-9400.

[12] O. Trabelsi, F.M. Davis, J.F. Rodriguez-Matas, A. Duprey, S. Avril, Patient specific stress and rupture analysis of ascending thoracic aneurysms, J Biomech, 48 (2015) 1836-1843.

[13] A.K. Venkatasubramaniam, M.J. Fagan, T. Mehta, K.J. Mylankal, B. Ray, G. Kuhan, I.C. Chetter, P.T. McCollum, A comparative study of aortic wall stress using finite element analysis for ruptured and non-ruptured abdominal aortic aneurysms, European Journal of Vascular and Endovascular Surgery, 28 (2004) 168-176.

[14] L. Liang, M. Liu, C. Martin, J.A. Elefteriades, W. Sun, A machine learning approach to investigate the relationship between shape features and numerically predicted risk of ascending aortic aneurysm, Biomech Model Mechanobiol, 16 (2017) 1519-1533.

[15] S. Pasta, G. Gentile, G.M. Raffa, D. Bellavia, G. Chiarello, R. Liotta, A. Luca, C. Scardulla, M. Pilato, In Silico Shear and Intramural Stresses are Linked to Aortic Valve Morphology in Dilated Ascending Aorta, European journal of vascular and endovascular surgery : the official journal of the European Society for Vascular Surgery, 54 (2017) 254-263.

[16] A. Rinaudo, S. Pasta, Regional variation of wall shear stress in ascending thoracic aortic aneurysms, Proceedings of the Institution of Mechanical Engineers. Part H, Journal of engineering in medicine, 228 (2014) 627-638.

[17] J.J. Lee, G. D'Ancona, A. Amaducci, F. Follis, M. Pilato, S. Pasta, Role of computational modeling in thoracic aortic pathology: a review, J Card Surg, 29 (2014) 653-662.

[18] G. D'Ancona, A. Amaducci, A. Rinaudo, S. Pasta, F. Follis, M. Pilato, R. Baglini, Haemodynamic predictors of a penetrating atherosclerotic ulcer rupture using fluid-structure interaction analysis, Interactive cardiovascular and thoracic surgery, 17 (2013) 576-578.

[19] A.J. Barker, C. Lanning, R. Shandas, Quantification of Hemodynamic Wall Shear Stress in Patients with Bicuspid Aortic Valve Using Phase-Contrast MRI, Annals of Biomedical Engineering, 38 (2010) 788-800.

[20] S. Pasta, V. Agnese, M. Di Giuseppe, G. Gentile, G.M. Raffa, D. Bellavia, M. Pilato, In Vivo Strain Analysis of Dilated Ascending Thoracic Aorta by ECG-Gated CT Angiographic Imaging, Annals of biomedical engineering, 45 (2017) 2911-2920.

[21] H. Haraldsson, M. Hope, G. Acevedo-Bolton, E. Tseng, X. Zhong, F.H. Epstein, L. Ge, D. Saloner, Feasibility of asymmetric stretch assessment in the ascending aortic wall with DENSE cardiovascular magnetic resonance, J Cardiovasc Magn Reson, 16 (2014) 6.

[22] G.R. Joldes, K. Miller, A. Wittek, B. Doyle, A simple, effective and clinically applicable method to compute abdominal aortic aneurysm wall stress, J Mech Behav Biomed Mater, 58 (2016) 139-148.

[23] M. Liu, L. Liang, W. Sun, A new inverse method for estimation of in vivo mechanical properties of the aortic wall, J Mech Behav Biomed Mater, 72 (2017) 148-158.

[24] S. Farzaneh, O. Trabelsi, S. Avril, Inverse identification of local stiffness across ascending thoracic aortic aneurysms, Biomech Model Mechanobiol, (2018).

[25] L. Liang, M. Liu, C. Martin, W. Sun, A deep learning approach to estimate stress distribution: a fast and accurate surrogate of finite-element analysis, J R Soc Interface, 15 (2018).

[26] B.J. Doyle, P.E. Norman, P.R. Hoskins, D.E. Newby, M.R. Dweck, Wall Stress and Geometry of the Thoracic Aorta in Patients With Aortic Valve Disease, Ann Thorac Surg, 105 (2018) 1077-1085.

[27] V. Mendez, M. Di Giuseppe, S. Pasta, Comparison of hemodynamic and structural indices of ascending thoracic aortic aneurysm as predicted by 2-way FSI, CFD rigid wall simulation and patient-specific displacement-based FEA, Computers in Biology and Medicine, 100 (2018) 221-229.

[28] K. Miller, J. Lu, On the prospect of patient-specific biomechanics without patient-specific properties of tissues, J Mech Behav Biomed Mater, 27 (2013) 154-166.

[29] J. Lu, X.L. Zhou, M.L. Raghavan, Inverse method of stress analysis for cerebral aneurysms, Biomechanics and Modeling in Mechanobiology, 7 (2008) 477-486.

[30] G.A. Holzapfel, T.C. Gasser, R.W. Ogden, A new constitutive framework for arterial wall mechanics and a comparative study of material models, Journal of Elasticity, 61 (2000) 1-48.

[31] S. Pasta, J.A. Phillippi, A. Tsamis, A. D'Amore, G.M. Raffa, M. Pilato, C. Scardulla, S.C. Watkins, W.R. Wagner, T.G. Gleason, D.A. Vorp, Constitutive modeling of ascending thoracic aortic aneurysms using microstructural parameters, Med Eng Phys, 38 (2016) 121-130.

[32] A.N. Azadani, S. Chitsaz, A. Mannion, A. Mookhoek, A. Wisneski, J.M. Guccione, M.D. Hope, L. Ge, E.E. Tseng, Biomechanical properties of human ascending thoracic aortic aneurysms, Ann Thorac Surg, 96 (2013) 50-58.

[33] S. Pasta, A. Rinaudo, A. Luca, M. Pilato, C. Scardulla, T.G. Gleason, D.A. Vorp, Difference in hemodynamic and wall stress of ascending thoracic aortic aneurysms with bicuspid and tricuspid aortic valve, J Biomech, 46 (2013) 1729-1738.

[34] D.P. Nathan, C. Xu, J.H. Gorman III, R.M. Fairman, J.E. Bavaria, R.C. Gorman, K.B. Chandran, B.M. Jackson, Pathogenesis of acute aortic dissection: a finite element stress analysis, Ann Thorac Surg, 91 (2011) 458-463.

[35] G. Martufi, T.C. Gasser, J.J. Appoo, E.S. Di Martino, Mechano-biology in the thoracic aortic aneurysm: a review and case study, Biomech Model Mechanobiol, 13 (2014) 917-928.

[36] J.E. Zelaya, S. Goenezen, P.T. Dargon, A.F. Azarbal, S. Rugonyi, Improving the efficiency of abdominal aortic aneurysm wall stress computations, Plos One, 9 (2014) e101353.

[37] J. Biehler, M.W. Gee, W.A. Wall, Towards efficient uncertainty quantification in complex and large-scale biomechanical problems based on a Bayesian multi-fidelity scheme, Biomech Model Mechanobiol, 14 (2015) 489-513.

[38] O. Trabelsi, A. Duprey, J.P. Favre, S. Avril, Predictive Models with Patient Specific Material Properties for the Biomechanical Behavior of Ascending Thoracic Aneurysms, Ann Biomed Eng, 44 (2016) 84-98.

[39] A. Wittek, K. Karatolios, C.P. Fritzen, J. Bereiter-Hahn, B. Schieffer, R. Moosdorf, S. Vogt, C. Blase, Cyclic three-dimensional wall motion of the human ascending and abdominal aorta characterized by time-resolved three-dimensional ultrasound speckle tracking, Biomech Model Mechanobiol, 15 (2016) 1375-1388.

[40] M. Peirlinck, M. De Beule, P. Segers, N. Rebelo, A modular inverse elastostatics approach to resolve the pressure-induced stress state for in vivo imaging based cardiovascular modeling, J Mech Behav Biomed Mater, 85 (2018) 124-133.

[41] D.C. Iliopoulos, R.P. Deveja, E.P. Kritharis, D. Perrea, G.D. Sionis, K. Toutouzas, C. Stefanadis, D.P. Sokolis, Regional and directional variations in the mechanical properties of ascending thoracic aortic aneurysms, Medical Engineering & Physics, 31 (2009) 1-9.

[42] A.N. Azadani, S. Chitsaz, P.B. Matthews, N. Jaussaud, J. Leung, T. Tsinman, L. Ge, E.E. Tseng, Comparison of mechanical properties of human ascending aorta and aortic sinuses, Ann Thorac Surg, 93 (2012) 87-94.

554

Figure Legends

Figure 1: Equibiaxial raw stress-strain data for ATAA specimens in (A) circumferential (CIRC) and (B) longitudinal (LONG) directions; labels indicate specimens obtained from same patient

Figure 2: Representative distribution of circumferential strain for patient P.2 as obtained after optimization procedure and raw stress-strain data in the circumferential direction showing the range of strain.

Figure 3: Distribution of “almost-true” stress determined using a very stiff material for the aortic wall as compared to stress from the optimal material properties for the Yeoh and Fung constitutive models of P.1

Figure 4: Comparison of stress-strain response curves under equibiaxial loading condition for three representative patients as modeled with two-term Yeoh constitutive model (top row) and Fung-exponential model (bottom row) using experimental and optimized material parameters; dots indicates maximum value of peak systolic strain

Figure 5: Distribution of patients-specific stress as quantified by the maximum principal stress at peak systole for all patients using the Yeoh constitutive material formulation based on the fitting of experimental data.

Figure 6: Distribution of patients-specific stress as quantified by the maximum principal stress at peak systole for all patients using the Fung constitutive material formulation based on the fitting of experimental data.

Figure 7: Comparisons of stress distribution for P.3 using the material parameters obtained by the FEA using the statically-determinate optimization procedure versus the FEA using patient-specific material parameters.

Table 1: Patient demographic information

Patient ID	Age	Gender	Aortic Valve	Type	Systolic Diameter (mm)	Diastolic Diameter (mm)	Thickness (mm)
P.1	70	Male	BAV	AP	52.0	51.2	2.1
P.2	71	Male	TAV	/	50.4	50.8	1.9
P.3	67	Male	TAV	/	54.8	57.1	2.2
P.4	56	Male	BAV	RL	52.4	53.6	1.8
P.5	58	Male	TAV	/	42.3	45.2	2.2
P.6	67	Male	TAV	/	48.5	49.8	2.8
P.7	78	Male	TAV	/	46.5	47.8	2.1
P.8	63	Female	TAV	/	54.8	55.8	1.7
P.9	68	Male	TAV	/	44.7	45.1	2.3

584 **Table 2:** Constitutive material parameters as obtained by the fitting of experimental biaxial
585 testing (exp) and by the elastostatic optimization procedure (opt); coefficient of determination
586 (R^2) refer to experimental data
587

Patient ID		Yeoh			Fung				
		c_1^y (kPa)	c_2^y (kPa)	R^2	c_1^F	a_1	a_2	a_3	R^2
P.1	exp	13.1	147.9	0.990	5.6	6.7	6.6	4.7	0.970
	opt	21.6	157.5		27.1	13.8	8.7	5.5	
P.2	exp	31.1	42.6	0.990	29.9	32.3	53.2	12.4	0.984
	opt	38.6	43.1		112.1	8.9	8.2	7.5	
P.3	exp	64.9	134.5	0.980	42.0	15.4	1.0	1.4	0.990
	opt	84.2	35.4		110.0	4.4	15.2	8.2	
P.4	exp	38.4	101.1	0.990	55.8	3.1	10.6	0.1	0.991
	opt	27.0	169.7		6.6	1.2	2.4	0.5	
P.5	exp	75.6	884.0	0.970	14.5	29.2	31.1	1.7	0.982
	opt	50.1	560.0		4.5	12.02	13.1	12.6	
P.6	exp	50.4	75.1	0.998	32.8	8.1	12.7	1.2	0.978
	opt	96.4	42.1		96.8	14.3	12.4	4.8	
P.7	exp	3.8	86.7	0.990	99.7	2.5	3.8	-0.2	0.998
	opt	55.2	32.6		15.9	14.1	15.1	3.0	
P.8	exp	15.4	242.0	0.974	5.8	21.9	20.5	-7.8	0.935
	opt	51.2	480.9		42.1	26.3	26.2	-21.0	
P.9	exp	121.8	446.8	0.968	55.6	11.0	0	0.0	0.914
	opt	163.4	240.7		54.1	14.2	66.1	30.7	

588
589

Table 3: Range of strain determined from CT imaging (ε_{CIRC}) and corresponding yield strain (ε_{yield}) extrapolated from stress-strain raw data of biaxial testing.

	P.1		P.2		P.3		P.4		P.5		P.6		P.7		P.8		P.9	
	min	max	min	max	min	max	min	max	min	max	min	max	min	max	min	max	min	max
ε_{CIRC}	0.01	0.15	0.01	0.03	0.04	0.15	0.03	0.12	0.02	0.18	0.01	0.16	0.01	0.13	0.05	0.10	0.01	0.13
ε_{yield}	0.16		0.24		0.25		0.17		0.15		0.09		0.21		0.17		0.08	

Table 4: Mean absolute percentage error (MAPE) of maximum principal stress between experimentally-derived and optimized material parameters.

	P.1	P.2	P.3	P.4	P.5	P.6	P.7	P.8	P.9
Yeoh	0.7105	0.7398	0.7545	0.4520	0.5303	0.7034	0.2138	0.1754	0.3245
Fung	0.7683	0.1140	0.6022	0.3241	0.7539	0.7130	0.0349	0.2198	0.7034

*Revised manuscript (clean)
Click here to download Revised manuscript (clean): Inverse Problem_Rev6_CLEAN.docx

On the Role of Material Properties in Ascending Thoracic Aortic Aneurysms

Federica Cosentino[1,2], Valentina Agnese[3], Giuseppe M Raffa[3], Giovanni Gentile[3], Diego Bellavia[3], Massimiliano Zingales[4], Michele Pilato[3], Salvatore Pasta[2,3*]

[1] Biomedical Department of Internal Medicine and Specialities (DIBIMIS), Piazza delle Cliniche, n.2, 90128, University of Palermo, Palermo, Italy
[2] Fondazione Ri.MED, Via Bandiera n.11, 90133, Palermo, Italy;
[3] Department for the Treatment and Study of Cardiothoracic Diseases and Cardiothoracic Transplantation, IRCCS-ISMETT, Via Tricomi n.5, 90127, Palermo, Italy
[4] Department of Civil, Environmental, Aerospace, Materials Engineering (DICAM), Viale delle Scienze Ed.8, 90128, University of Palermo, Palermo, Italy

Conflict of interest: none

[*] Corresponding author:
Salvatore Pasta, PhD
Professor of Industrial Bioengineering,
Fondazione Ri.MED
Phone: +39 091 3815681
FAX: +39 091 3815682
e-mail: spasta@fondazionerimed.com

Abstract: One of the obstacles standing before the biomechanical analysis of an ascending thoracic aortic aneurysm (ATAA) is the difficulty in obtaining patient-specific material properties. This study aimed to evaluate differences on ATAA-related stress predictions resulting from the elastostatic analysis based on the optimization of arbitrary material properties versus the application of patient-specific material properties determined from *ex-vivo* biaxial testing. Specifically, the elastostatic analysis relies the on the fact that, if the aortic wall stress does not depend on material properties, the aorta has to be statistically determinate. Finite element analysis (FEA) was applied to a group of nine patients who underwent both angio-CT imaging to reconstruct ATAA anatomies and surgical repair of diseased aorta to collect tissue samples for experimental material testing. Tissue samples cut from excised ATAA rings were tested under equibiaxial loading conditions to obtain experimentally-derived material parameters by fitting stress-strain profiles. FEAs were carried out using both optimized and experimentally-derived material parameters to predict and compare the stress distribution using the mean absolute percentage error (MAPE). Although physiological strains were below yield point (range of 0.08-0.25), elastostatic analysis led to errors on the stress predictions that depended on the type of constitutive model (highest MAPE of 0.7545 for Yeoh model and 0.7683 for Fung model) and ATAA geometry (lowest MAPE of 0.0349 for patient P.7). Elastostatic analysis needs better understanding of its application for determining aneurysm mechanics, and patient-specific material parameters are essential for reliable accurate stress predictions in ATAAs.

Keywords: ascending aortic aneurysm; inverse approach, material parameters, aortic aneurysm failure, finite-element analysis

INTRODUCTION

A ruptured ascending thoracic aortic aneurysm (ATAA) is considered a surgical emergency since progressive dilatation is often fatal if this disease is not detected by diagnostic imaging and managed immediately [1]. Despite being a relatively rare event with an estimated incidence of 5.0 per 100,000 individuals per year, the risk of fatal complications such as rupture or acute dissections can be as high as 50% in patients with a large ATAA wall (aortic diameter >50mm) [2, 3]. The risk over time of ATAA development to a size of 40-45mm in patients with a congenital bicuspid aortic valve (BAV) versus the morphological normal tricuspid aortic valve (TAV) is remarkable. Several studies highlighted that 84% of individuals with BAV may develop aortopathy during the life course [4, 5]. With regards to ATAA, degenerative aneurysms tend to develop in the mid-ascending aorta and then progress distally and proximally while ATAAs associated with connective tissue disorders are usually confined to the aortic root [6].

Although the aortic size criterion can be adjusted to achieve higher patient specificity using the body surface area or patient height [7], the surgical dilemma still exists because fatal complications can occur at aortic diameters lower than that dictated by current clinical guidelines for elective repair of aneurysmal aorta [8]. There is a need to delineate additional metrics, not based on aortic size, to better identify the risk of ATAA failure. Biomechanical risk assessments using finite element analysis (FEA) to estimate the wall stress exerted on the diseased aorta have been proposed in abdominal aortic aneurysms [9] [10] and ATAAs [11, 12]. These approaches for risk stratification appeared to be promising since peak wall stress can be calculated from routinely performed CT scans and may be a better predictor of risk of rupture than aortic diameter [13]. Recently, FEA was combined with machine learning techniques to study the relationship between shape features and wall stress as risk metric of ATAA, towards the development of computer-aided-diagnosis [14].

FEAs depend on several factors including the aortic geometry, the loading condition induced by hemodynamic and structural loads and the material properties of aortic wall constituents. Hemodynamic can be evaluated by computational fluid dynamic [15-18] or *in-vivo* 4D flow MRI [19] while tracking algorithms of aortic wall surface detected by dynamic CT [20] or MRI [21] can be adopted to estimate the ATAA-related structural mechanics. Obtaining material parameters non-invasively during patient monitoring for preoperative risk estimations represent an important challenge. However, if the stress distribution does not depend on material properties, the structure has to be statically determinate [22,28]. Under this condition, we can eliminate the need for patient-specific material properties and the FEA can be performed with arbitrary material properties because they do not affect the resulting wall stress. Several research groups adopted this approach to compute wall stress of abdominal [22] and ascending aortic aneurysms [23-26].

In this proof-of-concept, we want to know how different would be the resulting stress distribution on the aneurysm wall if material properties derived by an elastostatic analysis proposed by Liu et al. [23] are used as compared to FEAs using patient-specific material properties determined from *ex-vivo* biaxial testing. If large differences of stress distributions are observed, one could raise a red flag for further investigation using this appealing approach. To accomplish this task, we carried out FEAs on nine patients who underwent both dynamic CT imaging and surgical elective repair of ATAA to both reconstruct aortic geometries for FEA and collect tissue samples for patient-specific material property evaluation by the fitting of experimental stress-strain curves. Both an isotropic- (ie, two-term Yeoh model) and an anisotropic (ie, Fung-exponential model) constitutive formulation were tested. A stress comparison using the optimal material set versus the experimentally-derived material set was performed, and results were discussed.

METHODS

Study Population

All nine patients included in this investigation had electrocardiogram-gated computed tomography angiography (ECG-gated CT) for the measurement of the maximum aortic diameter and then elective surgical repair of dilated aortas at ISMETT IRCCS hospital institution. ECG-gated CT scans were reconstructed to obtain images at both diastolic and systolic cardiac phases, which were used for the estimation of the diastolic-to-systolic displacement field of the aortic wall. This displacement field was used as a boundary condition for FEA as previously described by our group [27]. Aortic valve shape was classified as TAV versus BAV based on reconstructed images parallel to the aortic valve plane. The presence of the raphe was used to group BAV morphology according to the fusion of right and left cusps (AP) as well as the fusion of right and non-coronary cusp (RL). After surgical ATAA repair, excised aortic tissues were stored in a physiologic solution upon biaxial mechanical testing. Table 1 shows patient demographic information, pre-operative aortic diameters and thickness measurements. The study was approved by the local research ethics committee, and all patients signed informed consent prior enrollment.

Biaxial Testing

Experimentally-related material properties from aneurysmal tissue samples collected for each patient were estimated by equibiaxial mechanical testing using an ElectroForce TestBench system (TA Instrument, Boston, MA). In brief, square specimens (10x10mm) cut form the tissue region located along the major curvature of the aortic ring were extrapolated. Each specimen was oriented along longitudinal and circumferential directions of the aortic vessel while sutures were used to fix specimen edge using surgical staples. Thickness was measured with a caliper for each sample (see Table 1). Five black markers were placed on the intimal aortic tissue surface to evaluate engineering strains along testing directions using a digital video extensometer placed perpendicular to the testing area. During biaxial loading, the specimen

was sub-merged in 0.9% physiologic saline solution in a bath under controlled temperature of 37^{o}C. A small preload (0.5 grams) was set prior to the displacement-driven testing protocol and, after preconditioning, a constant speed of 1mm/min was applied to four electromagnetic motors for loading the specimen under equibiaxial condition. Two 200N load cells were used to record forces along material directions. Data analysis to obtain stress and strain were calculated as defined in the constitutive modeling section.

Constitutive Modeling

FEAs were carried out using two specific classes of materials: a) the isotropic Yeoh material model in the two-term formulation proposed by Raghavan and Vorp [9] for abdominal aortic aneurysms, and b) the orthotropic Fung-exponential model that is often used in soft tissue biomechanics. Both models adopt homogenous, incompressible and hyperplastic description of ATAA wall mechanics.

In short, the two-term Yeoh constitutive model relates the stress tenors (S) in the loaded specimen to the stretch (λ) through the equation:

$$S_{11} = S_{22} = \left[2\, c_1^{(Y)} + 4\, c_2^{(Y)}\, (\lambda^2 + 2\,\lambda^{-1} - 3)\right][\lambda^2 - \lambda^{-1}] \quad (1)$$

with $c_1^{(Y)}$ and $c_2^{(Y)}$ are material model parameters indicative of the mechanical properties of the ATAA wall, and λ is equal to the deformed specimen length divided by the original length. $S_{33} = 0$ according to the membrane stress state assumption adopted in our FEA approach.

The free energy function for the Fung model was:

$$f(\mathbf{C}) = \frac{c_1^{(F)}}{2}\left[\exp\left[Q(\mathbf{C})\right] - 1\right] \quad (2)$$

158 with $\left[c_1^{(F)}\right] = F/L$ the material-like parameter , $\mathbf{C} = \mathbf{F}^T\mathbf{F}$ the right Cauchy-Green strain tensor

159 while the material-dependent exponent, $Q(\boldsymbol{C})$, was a quadratic form of Cauchy-Green strain

160 tensor $\mathbf{C} = \mathbf{F}^T\mathbf{F}$:

161 $$Q(\mathbf{C}) = a_1 I_1^2 + a_2 I_2^2 + 2a_3 I_1 I_2 \quad (3)$$

162 with a_1, a_2, a_3 the dimensionless parameter.

163

164 The Cauchy stresses of Fung constitutive formulation are therefore expressed as:

$$\sigma_{11} = 2\lambda_1^2 c_1^{(F)} e^Q (a_1\lambda_1 + a_3\lambda_2)$$

$$\sigma_{22} = 2\lambda_2^2 c_1^{(F)} e^Q (a_3\lambda_1 + a_2\lambda_2) \quad (4\ a,b)$$

165 ***Constitutive Material Parameter Estimation***

166 The elastostatic analysis for the evaluation of material constitutive parameters proposed by Liu

167 et al [23] is based on the main premise for which the stress distribution is statically determinate.

168 Thus, for a given ATAA deformed configuration (ie, peak of systole) and known loading

169 condition (ie, the diastolic-to-systolic displacement field), different material parameters and

170 constitutive models will give nearly the same stress field. In this way, an “almost-true” stress

171 field at systole can be approximately obtained by an infinitesimal linear elastic model with

172 sufficiently stiff material parameters. This fact has been theoretically justified by Miller and Lu

173 [28] and numerically verified by Lu et al. [29] and Joldes et al. [22]. Given the constitutive model

174 with an initial guess of material parameters (ie, $c_1^{(Y)}$ and $c_2^{(Y)}$ for Yeoh model and $c_1^{(F)}$, a_1, a_2, a_3

175 for the Fung model), by using the constitutive equations and deformation relationship between

176 the two loading states, an optimization algorithm allows to find the “true” material parameters

177 such that the difference between the estimated and “almost-true” stress fields is minimized.

178 Thus, the objective of the optimization process was to find a set of material descriptors that

minimize the difference between the "almost-true" systolic stress, $\tilde{\sigma}^{t}$, and estimated systolic stress, $\tilde{\sigma}^{est}$, for each element as:

$$g_e^{(Y)} = \sum_{m=1}^{N}\sum_{i=1}^{2}\left[\tilde{S}_i^{(t)} - \tilde{S}_i^{(e)}\left(c_1^{(Y)}, c_2^{(Y)}\right)\right]^2$$
$$g_e^{(F)} = \sum_{m=1}^{N}\sum_{i=1}^{2}\left[\tilde{S}_i^{(t)} - \tilde{S}_i^{(F)}\left(c_1^{(F)}, a_1, a_2, a_3\right)\right]^2 \quad \text{(5 a,b)}$$

where N is the number of elements used in each model and i is the component index of each principal stress component. Eq. 1 and Eq. 4 were used for the estimated systolic stress of Yeoh and Fung models, respectively.

The optimization was implemented in the mathematical language program, MATLAB (v2018, Mathworks, MA, USA). Nonlinear least-squares algorithm with trust-region-reflective was used for the optimization of Yeoh material parameters using $c_1^{(Y)} > 0$ and $c_2^{(Y)} > 0$ as lower bounds. For the Fung-exponential form, physically meaningful and plausible material parameters were obtained by enforcing the convexity of the strain energy function and thus performing constrained minimization. For planar biaxial loading of soft tissue, strict convexity physically implies that the projections of the contour of $f(\mathbf{C})$ on the I_1 - I_2 plane form a convex surface [30]. It can be shown that if $c_1^{(F)} > 0$, then Eq. 4 is likely convex if and only if $a_1 > 0$, $a_2 > 0$ and $a_1\, a_2 - a_3^2 > 0$

For the estimation of the "almost-true" systolic stress distribution, we selected a very stiff material for the aortic wall (E=2x10^4 GPa and v=0.49) to obtain Cauchy stress. As initial guess of material descriptors, we used the population-average material properties reported by Pasta et al. [31] for the two-term Yeoh model and by Azdani et al. [32] for the Fung model of ATAAs. For

each optimization procedure, principal stresses were imported in MATALB by postprocessing of ABAQUS models, and the optimization was done to obtain the optimal material parameters.

Computational Study

ECG-gated CT images were used to segment the ATAA wall at both end-diastolic and peak-systolic cardiac phases using the medical imaging software Mimics (Mimics v20, Materialise, Leuven, BE) [15, 33]. Semi-automatic threshold-based segmentation of aortic lumen allowed us to obtain a point cloud (resolution of 0.3 mm), which was triangulated to generate a surface mesh of both diastolic and systolic ATAA geometries. Using an algorithm previously developed by our group in MATLAB (v2018, Mathworks, MA, USA), the point cloud of the diastolic aortic-luminal surface was projected normally onto the systolic aortic-luminal surface to determine the displacement field as the Euclidean distance between closest points [15]. The estimated diastolic-to-systolic displacement field was then implemented as a boundary condition in the FEA model for estimating wall stresses.

For each patient, FEAs were developed using the reconstructed ATAA geometry at diastole, which was meshed with quadrilateral (M3D4R) and triangular (M3D3) membrane elements in ABAQUS/Explicit (v2018, SIMULIA Inc, Providence, RI). Reduced integration was used for the 4-node quadrilateral membrane element. Grid convergence led to an element size of 0.7mm (element range of 28,200-37,500) to obtain a reproducible stress analysis of the human thoracic aorta [34]. Uniform material properties were adopted for the aortic wall while thickness measured from tissue samples was set for each patient simulation. Distal ends of the descending aorta and supra-aortic vessels were fixed in all directions. Material fiber direction was set using multiple cylindrical coordinate systems with origins in the centerline of the aneurysmal aorta. The ATAA wall was modeled using two constitute formulations to assess the

role of the isotropic- and anisotropic material behavior on the resulting stress distribution. The density of the aortic tissue was 1060 kg/m^3. In the Abaqus/Explicit solver, ATAA wall mechanics was modeled as a quasi-static process while the energy was monitored to ensure the ratio of kinetic energy to internal energy remains less than 10%. Adequate time step was applied while an element-by-element stable time increment estimate, coupled with a "variable mass scaling technique," reduced the computational cost of each simulation. Mass scaling was performed by scaling the masses of elements whose stable time increments was less than the user-supplied time increment of 1.e-7 s so that the element stable time increment for these elements becomes equal to the user-supplied time increment. This approach has a minor effect on the stress analysis.

The numerical strategy is here summarized:

1. For the estimation of the "almost-true" stress distribution, the FEA model of each patient was loaded with a uniform peak systolic pressure distribution of 120mmHg in a very stiff aortic wall (E=2x10^4 GPa and v=0.49). This approach led to infinitesimal deformation of aneurysmal aorta.
2. The resulting "almost-true" stress distribution was adopted to optimize the population-average material descriptors of Yeoh and Fung constitutive relationships. This step allowed us to find the optimal material parameters specific to a given patient geometry.
3. A second set of simulations was performed using the optimal material properties and the diastolic-to-systolic displacement field (instead of the uniform pressure distribution) to find realistic deformation of ATAA wall.
4. A third set of simulations was carried out using the displacement field as the boundary condition but using the experimental material properties evaluated from *ex-vivo* material testing. Then, results were compared to those observed for the second set of simulations.

RESULTS

Experimental biaxial testing

Experimental raw data from equibiaxial testing are shown as Piola-Kirchhoff stress versus engineering-strain plots for ATAAs in both circumferential and longitudinal directions of ascending aorta (Figure 1). Most of stress-strain data presented a linear part, related to the elastic properties of the aneurysmal aortic tissue, followed by an exponential part related to the collagen fiber recruitment. These parts were separated by the “yield point”, which is more likely to define the *in-vivo* stress range. For a given tissue specimen, there was no remarkable difference of material response between longitudinal and circumferential directions, suggesting isotropic mechanical behavior for ATAA wall as previously found [31]. Stress-strain data were successfully fit by both the isotropic and anisotropic constitutive models, and the material parameters for each patient were estimated (Table 2). Fitting was able to accurately reproduce the non-linear behavior of experimental data (R^2>0.91 in all cases) so that material descriptors can be considered as determinants of the biomechanical behavior of ATAA wall. After running the elastostatic optimization analysis, material parameters were found close to those obtained from the fitting of the experimental stress-strain curves. We observed that even a variation of 10% on the initial guess of the constitutive parameter set did not determine remarkable changes on the optimal material parameters.

Strain analysis

Figure 2 shows the distribution of diastolic-to-systolic strain field as well as the experimental stress-strain curve from biaxial testing of the aortic tissue specimen cut from the same patient. It can be observed that the range of “true” strain in the circumferential direction is below the yield strain, which is the value of the strain at yield point before reaching the steep increase in the stress-strain response of tested aortic tissue specimen. Most of patients experienced low strain

at CT imaging, except for patients P.6 and P.9 who experience strains remarkably above the yield strain (Table 3). This can be determined by high blood pressure induced by hypertension, increased stretch and twist of aortic vessel due to heart beating and local changes of material properties or tissue thickness, exposing the aneurysmal aorta at greater risk of complications than other patients.

"Almost-true" stress computation

The distribution of "almost-true" stress determined by the simple linear-elastic FEA with the stiff elastic modulus was compared to that obtained at the end of optimization procedure for each patient simulation. Specifically, the maximum principal stress exerted on the ATAA wall was used as an indicator of intramural stress of aneurysmal aorta. Figure 3 shows that the stiff ATAA model had a stress distribution similar to that of Fung model but different from that shown by the Yeoh model. The mean absolute percentage error (MAPE) was calculated for each patient as a measure of differences among simulation approaches. For the patient P.1 shown in Figure 3, the MAPE was nearly 30% between the "almost-true" and Yeoh models and 8.5% between the "almost-true" and Fung models. For other patient cases, we found errors in the range of 6-18%.

Biaxial testing of optimal vs experimental material parameters

Optimized material parameters obtained from elastostatic analysis were used to determine the stress-strain response under equibiaxial loading conditions in a FEA reproducing the experimental testing of aortic tissue sample. Then, the stress-strain curves were plotted together with the experimental testing data (see Figure 4). P.2 with small strain field exhibited a practically equivalent stress-strain response with both experimental and elastostatic material descriptors. At strain of 14%, P.6 had the largest discrepancy of 24% in stress predictions between optimized and experimental material descriptors of two-term Yeoh constitutive model.

Patient-specific FEA of optimal vs experimental material parameters

Figure 5 illustrates predicted wall stress distributions computed by patient-specific material descriptors determined from experimental biaxial testing of Yeoh model. Local maxima of wall stress were mainly placed near the maximum curvature of the ascending aorta, just above the sino-tubular junction. In a similar way, Figure 6 shows predicted wall stress maps resulting from the experimentally-based material fitting using the Fung model. It can be observed that stress distributions are similar among constitutive formulations (ie, Yeoh versus Fung model) when patient-specific material parameters are adopted.

Although biaxial testing results of optimal versus experimental material parameters are encouraging, we found considerable discrepancies for the patient-specific stress predictions between the optimal material parameter set versus the experimentally-derived set (Figure 7). The MAPE was calculated for each patient and evinced highly variable differences from patient to patient and the type of constitutive formulation (see Table 4).

DISCUSSION

In this study, we exploited the appealing concept of obtaining reasonably and accurate stress solutions of aneurysm mechanics using an inverse approach, and thus without invoking accurate material descriptors that are hard to know before surgical management of ATAAs. We optimized population-average material parameters with respect to an “the “almost-true” stress fields obtained with an infinitesimal linear-elastic model based on a sufficiently stiff Young modulus [23]. The so-recovered material parameters were implemented in FEAs, and then stress distributions of nine ATAA geometries were compared to those predicted when patient-specific material descriptors are estimated from the fitting of *ex-vivo* testing data of aortic tissue specimens collected from the same patient. We observed that the stress-strain response under equibiaxial loading predicted by the elastostatic analysis was consistent to the experimental

material behavior if strain was low (largest difference of 24% at strain of 14%). This was in agreement with findings documented by Liu et al. [23]. However, the discrepancy on predicted stress distributions was considerably, depending on the adopted constitutive model and ATAA shape, when FEAs were performed on patient anatomies. Although the stress analysis of abdominal aortic aneurysms did not depend on material properties [22], the modeling of the ascending aorta as a statically-determinate structure needs further understanding so that the role of material properties is still important for realistic and accurate stress predictions.

Identification of patient-specific material parameters of ATAAs deserves important interest as FEAs rely on population-average values of material properties for those patients undergoing close monitoring of the aneurysm size. In risk predictions of aneurysm failure, FEAs based on patient-specific material descriptors were carried out in very few studies restricted to patients who underwent elective surgical repair of ATAA wall to derive the material behavior from uniaxial or bulge inflation tests [11, 12]. The role of material properties in computational growth and remodeling analyses may be even more remarkable as stress estimations are strongly dependents on local material changes [35].

To avoid *ex-vivo* material testing, inverse approaches allows to estimate material descriptors; however, inverse analysis involves a complex non-linear problem [36, 37]. Most of inverse techniques proposed for soft tissue mechanics attempt to minimize a cost function defined by the difference between a target parameter, which is determined from medical image analysis, and a candidate parameter estimated from FEA and then iteratively adjusted to tune material parameters of interest [38]. However, inverse approaches are commonly time consuming due to continuous interaction with the FEA solver [39]. For the ascending aorta, Trabelsi et al. [38] proposed an inverse method in which the target variable was the volume variation of the aorta measured from ECG-gated CT scans. They assumed a linear relationship between the

constitutive material parameter and the volume of the aortic luminal surface, and then carried out eight FEA analyses for each patient to build datasets for several CT measurements of ATAA volume at systole and mid-cardiac phase. The error attributed to this approach was 0.6% on estimated CT volume and 9.6% on the predicted stress response under equibiaxial test simulations. In agreement with our findings, the statically determinate inverse approach proposed by Liu et al. [23] for the Gasser-Holzapfel-Ogden constitutive model demonstrated comparable biaxial stress-strain curves between elastostatic analyses and experimental tests estimated in a previous investigation of the same group [11]. In their patient study group, patient-specific FEAs on ATAA anatomies were not done because of lack of both CT and tissue data, without quantification of stress changes computed with either experimental or elastostatic-based material parameters.

Generally, the stress of a deformable body depends not only on its geometry, load and boundary conditions, but also on the mechanical properties of constituents. One of the obstacles standing before the biomechanics community is the difficulty in obtaining patient-specific properties of tissues given the absence of a methodology to non-invasively estimate stress *in-vivo*. Notwithstanding, there is an emerging interest from several groups in reformulating computational mechanics in a new paradigm so that computational stress predictions are weakly sensitive to the variation of mechanical properties when the deformed configuration is given [28]. This paradigm can apply to non-linear elastic material, because the stress in such material depends on the relative deformation among two definite configurations. If one of them is known, the other can be solved from equilibrium, which is dominated by in-plane stress for thin-walled structure treated as a membrane. From the analysis of ECG-gated CT images, we observed that strain at deformed configuration bears to the linear-elastic part of the experimental stress-strain response (see Table 3), thereby supporting in part the static determinacy of the aneurysmal wall. In this way, the inverse problem can be directly formulated

using the constitutive law as here presented or shown by other studies [23, 40] and without the need of a continuous interaction with the FEA solver. Using the Fung model, Miller et al. [28] investigated the sensitivity of the stress solution with respect to material parameters and constitutive model in three intracranial aneurysm geometries under static determinacy. The inverse stress solution was far less sensitive to material description as, for instance, the 100 times increase in the stiffness parameter C of the Fung model led to a 2.9% error in the maximum principal stress prediction. As compared to abdominal or cerebral aneurysms, the ascending aorta is cyclically stretched and twisted every heartbeat by determining the presence of longitudinal and shear stresses in a way that the static equilibrium is not only governed by the internal pressure. These mechanical forces are also highly dynamic (as systole is approximately 0.33s), thereby determining viscoelastic effects. These factors combined to residual stress likely occurring in blood vessels can pose several doubts on the modeling of the ascending aorta as statically-determinate structure.

The major limitation of this study is that comparisons of stress predictions were carried out assuming the experimentally-derived material parameters as the true material descriptors of the ATAA wall, but these can be indeed different from the *in-vivo* condition. However, there is no methodology to *in-vivo* estimate the material behavior so that experimental material parameters are the most accurate ATAA material descriptors. FEAs were based on homogenous thickness and material properties for the whole aorta but there exist evidence of regional changes in the material properties and thickness along the vessel circumference [41] and from the aortic root to the distal ascending aorta [42]. It should be mentioned that the optimization procedure can be modified to account for heterogenous thickness and regionally-dependent material properties by slightly altering the workflow and evaluating the objective function element-by-element. Disregarding the presence of residual stresses and considering the arterial wall as a 3D membrane with uniform thickness can be considered as additional limitations of the current

406 work. It was assumed that the aortic wall behaves as a membrane with no bending moments or
407 no through thickness shear, although regions near the branches may not satisfy the membrane
408 assumption. The orientation of elastic fiber was not considered in FEAs, and this may alter the
409 stress distribution as demonstrated in a previous study [31]. Caliper-based measurements of
410 tissue thickness can lead to errors which in turn affect aortic wall stress predictions.
411
412 **CONCLUSION**
413 We conclude that the modeling of the ascending aorta as a statically determinate can lead to
414 errors on wall stress predictions in patient-specific FEAs since aortic wall stress was found to
415 depend on the type of constitutive model and ATAA geometry. Static determinacy needs better
416 understanding of its application to determine ascending aortic aneurysm mechanics so that
417 patient-specific material descriptors as determined by *ex-vivo* material testing are advocated for
418 reliable accurate stress predictions of ATAA wall mechanics.
419
420 **ACKNOWLEDGMENTS**
421 This work was supported by a “Ricerca Finalizzata” grant from the Italian Ministry of Health (GR-
422 2011-02348129) as well as by a grant from Fondazione RiMED to Salvatore Pasta. Federica
423 Cosentino thanks the Fondazione RiMED and Ministry of Education, University and Research
424 (MIUR) for supporting her PhD programme.

REFERENCES

[1] L.K. Bickerstaff, P.C. Pairolero, L.H. Hollier, L.J. Melton, H.J. Van Peenen, K.J. Cherry, J.W. Joyce, J.T. Lie, Thoracic aortic aneurysms: a population-based study, Surgery, 92 (1982) 1103-1108.

[2] M.A. Coady, J.A. Rizzo, G.L. Hammond, D. Mandapati, U. Darr, G.S. Kopf, J.A. Elefteriades, O.W. Isom, F. Robicsek, R.B. Griepp, What is the appropriate size criterion for resection of thoracic aortic aneurysms?, Journal of Thoracic and Cardiovascular Surgery, 113 (1997) 476-491.

[3] J.A. Beckman, Aortic aneurysms: pathophysiology, epidemiology and prognosis, in: M.A. Creager, V.J. Dzau, J. Loscalzo (Eds.) (eds): Vascular Medicine, Saunders Elsevier, Philadelphia, PA, 2006.

[4] S. Verma, S.C. Siu, Aortic dilatation in patients with bicuspid aortic valve, N Engl J Med, 370 (2014) 1920-1929.

[5] M.A. Borger, P.W.M. Fedak, E.H. Stephens, T.G. Gleason, E. Girdauskas, J.S. Ikonomidis, A. Khoynezhad, S.C. Siu, S. Verma, M.D. Hope, D.E. Cameron, D.F. Hammer, J.S. Coselli, M.R. Moon, T.M. Sundt, A.J. Barker, M. Markl, A. Della Corte, H.I. Michelena, J.A. Elefteriades, The American Association for Thoracic Surgery consensus guidelines on bicuspid aortic valve-related aortopathy: Full online-only version, J Thorac Cardiovasc Surg, 156 (2018) e41-e74.

[6] A. Della Corte, C. Bancone, C. Quarto, G. Dialetto, F.E. Covino, M. Scardone, G. Caianiello, M. Cotrufo, Predictors of ascending aortic dilatation with bicuspid aortic valve: a wide spectrum of disease expression, Eur J Cardiothorac Surg, 31 (2007) 397-404; discussion 404-395.

[7] J.A. Elefteriades, E.A. Farkas, Thoracic aortic aneurysm clinically pertinent controversies and uncertainties, J Am Coll Cardiol, 55 (2010) 841-857.

[8] L.A. Pape, T.T. Tsai, E.M. Isselbacher, J.K. Oh, P.T. O'Gara, A. Evangelista, R. Fattori, G. Meinhardt, S. Trimarchi, E. Bossone, T. Suzuki, J.V. Cooper, J.B. Froehlich, C.A. Nienaber, K.A. Eagle, Aortic diameter >= 5.5 cm is not a good predictor of type A aortic dissection - Observations from the international registry of acute aortic dissection (IRAD), Circulation, 116 (2007) 1120-1127.

[9] M.L. Raghavan, D.A. Vorp, Toward a biomechanical tool to evaluate rupture potential of abdominal aortic aneurysm: identification of a finite strain constitutive model and evaluation of its applicability, Journal of Biomechanics, 33 (2000) 475-482.

[10] M.F. Fillinger, S.P. Marra, M.L. Raghavan, F.E. Kennedy, Prediction of rupture risk in abdominal aortic aneurysm during observation: Wall stress versus diameter, J Vasc Surg, 37 (2003) 724-732.

[11] C. Martin, W. Sun, T. Pham, J. Elefteriades, Predictive biomechanical analysis of ascending aortic aneurysm rupture potential, Acta Biomater, 9 (2013) 9392-9400.

[12] O. Trabelsi, F.M. Davis, J.F. Rodriguez-Matas, A. Duprey, S. Avril, Patient specific stress and rupture analysis of ascending thoracic aneurysms, J Biomech, 48 (2015) 1836-1843.

[13] A.K. Venkatasubramaniam, M.J. Fagan, T. Mehta, K.J. Mylankal, B. Ray, G. Kuhan, I.C. Chetter, P.T. McCollum, A comparative study of aortic wall stress using finite element analysis for ruptured and non-ruptured abdominal aortic aneurysms, European Journal of Vascular and Endovascular Surgery, 28 (2004) 168-176.

[14] L. Liang, M. Liu, C. Martin, J.A. Elefteriades, W. Sun, A machine learning approach to investigate the relationship between shape features and numerically predicted risk of ascending aortic aneurysm, Biomech Model Mechanobiol, 16 (2017) 1519-1533.

[15] S. Pasta, G. Gentile, G.M. Raffa, D. Bellavia, G. Chiarello, R. Liotta, A. Luca, C. Scardulla, M. Pilato, In Silico Shear and Intramural Stresses are Linked to Aortic Valve Morphology in Dilated Ascending Aorta, European journal of vascular and endovascular surgery : the official journal of the European Society for Vascular Surgery, 54 (2017) 254-263.

[16] A. Rinaudo, S. Pasta, Regional variation of wall shear stress in ascending thoracic aortic aneurysms, Proceedings of the Institution of Mechanical Engineers. Part H, Journal of engineering in medicine, 228 (2014) 627-638.

[17] J.J. Lee, G. D'Ancona, A. Amaducci, F. Follis, M. Pilato, S. Pasta, Role of computational modeling in thoracic aortic pathology: a review, J Card Surg, 29 (2014) 653-662.

[18] G. D'Ancona, A. Amaducci, A. Rinaudo, S. Pasta, F. Follis, M. Pilato, R. Baglini, Haemodynamic predictors of a penetrating atherosclerotic ulcer rupture using fluid-structure interaction analysis, Interactive cardiovascular and thoracic surgery, 17 (2013) 576-578.

[19] A.J. Barker, C. Lanning, R. Shandas, Quantification of Hemodynamic Wall Shear Stress in Patients with Bicuspid Aortic Valve Using Phase-Contrast MRI, Annals of Biomedical Engineering, 38 (2010) 788-800.

[20] S. Pasta, V. Agnese, M. Di Giuseppe, G. Gentile, G.M. Raffa, D. Bellavia, M. Pilato, In Vivo Strain Analysis of Dilated Ascending Thoracic Aorta by ECG-Gated CT Angiographic Imaging, Annals of biomedical engineering, 45 (2017) 2911-2920.

[21] H. Haraldsson, M. Hope, G. Acevedo-Bolton, E. Tseng, X. Zhong, F.H. Epstein, L. Ge, D. Saloner, Feasibility of asymmetric stretch assessment in the ascending aortic wall with DENSE cardiovascular magnetic resonance, J Cardiovasc Magn Reson, 16 (2014) 6.

[22] G.R. Joldes, K. Miller, A. Wittek, B. Doyle, A simple, effective and clinically applicable method to compute abdominal aortic aneurysm wall stress, J Mech Behav Biomed Mater, 58 (2016) 139-148.

[23] M. Liu, L. Liang, W. Sun, A new inverse method for estimation of in vivo mechanical properties of the aortic wall, J Mech Behav Biomed Mater, 72 (2017) 148-158.

[24] S. Farzaneh, O. Trabelsi, S. Avril, Inverse identification of local stiffness across ascending thoracic aortic aneurysms, Biomech Model Mechanobiol, (2018).

[25] L. Liang, M. Liu, C. Martin, W. Sun, A deep learning approach to estimate stress distribution: a fast and accurate surrogate of finite-element analysis, J R Soc Interface, 15 (2018).

[26] B.J. Doyle, P.E. Norman, P.R. Hoskins, D.E. Newby, M.R. Dweck, Wall Stress and Geometry of the Thoracic Aorta in Patients With Aortic Valve Disease, Ann Thorac Surg, 105 (2018) 1077-1085.

[27] V. Mendez, M. Di Giuseppe, S. Pasta, Comparison of hemodynamic and structural indices of ascending thoracic aortic aneurysm as predicted by 2-way FSI, CFD rigid wall simulation and patient-specific displacement-based FEA, Computers in Biology and Medicine, 100 (2018) 221-229.

[28] K. Miller, J. Lu, On the prospect of patient-specific biomechanics without patient-specific properties of tissues, J Mech Behav Biomed Mater, 27 (2013) 154-166.

[29] J. Lu, X.L. Zhou, M.L. Raghavan, Inverse method of stress analysis for cerebral aneurysms, Biomechanics and Modeling in Mechanobiology, 7 (2008) 477-486.

[30] G.A. Holzapfel, T.C. Gasser, R.W. Ogden, A new constitutive framework for arterial wall mechanics and a comparative study of material models, Journal of Elasticity, 61 (2000) 1-48.

[31] S. Pasta, J.A. Phillippi, A. Tsamis, A. D'Amore, G.M. Raffa, M. Pilato, C. Scardulla, S.C. Watkins, W.R. Wagner, T.G. Gleason, D.A. Vorp, Constitutive modeling of ascending thoracic aortic aneurysms using microstructural parameters, Med Eng Phys, 38 (2016) 121-130.

[32] A.N. Azadani, S. Chitsaz, A. Mannion, A. Mookhoek, A. Wisneski, J.M. Guccione, M.D. Hope, L. Ge, E.E. Tseng, Biomechanical properties of human ascending thoracic aortic aneurysms, Ann Thorac Surg, 96 (2013) 50-58.

[33] S. Pasta, A. Rinaudo, A. Luca, M. Pilato, C. Scardulla, T.G. Gleason, D.A. Vorp, Difference in hemodynamic and wall stress of ascending thoracic aortic aneurysms with bicuspid and tricuspid aortic valve, J Biomech, 46 (2013) 1729-1738.

[34] D.P. Nathan, C. Xu, J.H. Gorman III, R.M. Fairman, J.E. Bavaria, R.C. Gorman, K.B. Chandran, B.M. Jackson, Pathogenesis of acute aortic dissection: a finite element stress analysis, Ann Thorac Surg, 91 (2011) 458-463.

[35] G. Martufi, T.C. Gasser, J.J. Appoo, E.S. Di Martino, Mechano-biology in the thoracic aortic aneurysm: a review and case study, Biomech Model Mechanobiol, 13 (2014) 917-928.

[36] J.E. Zelaya, S. Goenezen, P.T. Dargon, A.F. Azarbal, S. Rugonyi, Improving the efficiency of abdominal aortic aneurysm wall stress computations, Plos One, 9 (2014) e101353.

[37] J. Biehler, M.W. Gee, W.A. Wall, Towards efficient uncertainty quantification in complex and large-scale biomechanical problems based on a Bayesian multi-fidelity scheme, Biomech Model Mechanobiol, 14 (2015) 489-513.

[38] O. Trabelsi, A. Duprey, J.P. Favre, S. Avril, Predictive Models with Patient Specific Material Properties for the Biomechanical Behavior of Ascending Thoracic Aneurysms, Ann Biomed Eng, 44 (2016) 84-98.

[39] A. Wittek, K. Karatolios, C.P. Fritzen, J. Bereiter-Hahn, B. Schieffer, R. Moosdorf, S. Vogt, C. Blase, Cyclic three-dimensional wall motion of the human ascending and abdominal aorta characterized by time-resolved three-dimensional ultrasound speckle tracking, Biomech Model Mechanobiol, 15 (2016) 1375-1388.

[40] M. Peirlinck, M. De Beule, P. Segers, N. Rebelo, A modular inverse elastostatics approach to resolve the pressure-induced stress state for in vivo imaging based cardiovascular modeling, J Mech Behav Biomed Mater, 85 (2018) 124-133.

[41] D.C. Iliopoulos, R.P. Deveja, E.P. Kritharis, D. Perrea, G.D. Sionis, K. Toutouzas, C. Stefanadis, D.P. Sokolis, Regional and directional variations in the mechanical properties of ascending thoracic aortic aneurysms, Medical Engineering & Physics, 31 (2009) 1-9.

[42] A.N. Azadani, S. Chitsaz, P.B. Matthews, N. Jaussaud, J. Leung, T. Tsinman, L. Ge, E.E. Tseng, Comparison of mechanical properties of human ascending aorta and aortic sinuses, Ann Thorac Surg, 93 (2012) 87-94.

552

Figure Legends

Figure 1: Equibiaxial raw stress-strain data for ATAA specimens in (A) circumferential (CIRC) and (B) longitudinal (LONG) directions; labels indicate specimens obtained from same patient

Figure 2: Representative distribution of circumferential strain for patient P.2 as obtained after optimization procedure and raw stress-strain data in the circumferential direction showing the range of strain.

Figure 3: Distribution of “almost-true” stress determined using a very stiff material for the aortic wall as compared to stress from the optimal material properties for the Yeoh and Fung constitutive models of P.1

Figure 4: Comparison of stress-strain response curves under equibiaxial loading condition for three representative patients as modeled with two-term Yeoh constitutive model (top row) and Fung-exponential model (bottom row) using experimental and optimized material parameters; dots indicates maximum value of peak systolic strain

Figure 5: Distribution of patients-specific stress as quantified by the maximum principal stress at peak systole for all patients using the Yeoh constitutive material formulation based on the fitting of experimental data.

Figure 6: Distribution of patients-specific stress as quantified by the maximum principal stress at peak systole for all patients using the Fung constitutive material formulation based on the fitting of experimental data.

Figure 7: Comparisons of stress distribution for P.3 using the material parameters obtained by the FEA using the statically-determinate optimization procedure versus the FEA using patient-specific material parameters.

Table 1: Patient demographic information

Patient ID	Age	Gender	Aortic Valve	Type	Systolic Diameter (mm)	Diastolic Diameter (mm)	Thickness (mm)
P.1	70	Male	BAV	AP	52.0	51.2	2.1
P.2	71	Male	TAV	/	50.4	50.8	1.9
P.3	67	Male	TAV	/	54.8	57.1	2.2
P.4	56	Male	BAV	RL	52.4	53.6	1.8
P.5	58	Male	TAV	/	42.3	45.2	2.2
P.6	67	Male	TAV	/	48.5	49.8	2.8
P.7	78	Male	TAV	/	46.5	47.8	2.1
P.8	63	Female	TAV	/	54.8	55.8	1.7
P.9	68	Male	TAV	/	44.7	45.1	2.3

582 **Table 2:** Constitutive material parameters as obtained by the fitting of experimental biaxial
583 testing (exp) and by the elastostatic optimization procedure (opt); coefficient of determination
584 (R^2) refer to experimental data
585

Patient ID		Yeoh			Fung				
		c_1^y (kPa)	c_2^y (kPa)	R^2	c_1^F	a_1	a_2	a_3	R^2
P.1	exp	13.1	147.9	0.990	5.6	6.7	6.6	4.7	0.970
	opt	21.6	157.5		27.1	13.8	8.7	5.5	
P.2	exp	31.1	42.6	0.990	29.9	32.3	53.2	12.4	0.984
	opt	38.6	43.1		112.1	8.9	8.2	7.5	
P.3	exp	64.9	134.5	0.980	42.0	15.4	1.0	1.4	0.990
	opt	84.2	35.4		110.0	4.4	15.2	8.2	
P.4	exp	38.4	101.1	0.990	55.8	3.1	10.6	0.1	0.991
	opt	27.0	169.7		6.6	1.2	2.4	0.5	
P.5	exp	75.6	884.0	0.970	14.5	29.2	31.1	1.7	0.982
	opt	50.1	560.0		4.5	12.02	13.1	12.6	
P.6	exp	50.4	75.1	0.998	32.8	8.1	12.7	1.2	0.978
	opt	96.4	42.1		96.8	14.3	12.4	4.8	
P.7	exp	3.8	86.7	0.990	99.7	2.5	3.8	-0.2	0.998
	opt	55.2	32.6		15.9	14.1	15.1	3.0	
P.8	exp	15.4	242.0	0.974	5.8	21.9	20.5	-7.8	0.935
	opt	51.2	480.9		42.1	26.3	26.2	-21.0	
P.9	exp	121.8	446.8	0.968	55.6	11.0	0	0.0	0.914
	opt	163.4	240.7		54.1	14.2	66.1	30.7	

586
587

588 **Table 3:** Range of strain determined from CT imaging (ε_{CIRC}) and corresponding yield strain

589 (ε_{yield}) extrapolated from stress-strain raw data of biaxial testing.

590

	P.1		P.2		P.3		P.4		P.5		P.6		P.7		P.8		P.9	
	min	max	min	max	min	max	min	max	min	max	min	max	min	max	min	max	min	max
ε_{CIRC}	0.01	0.15	0.01	0.03	0.04	0.15	0.03	0.12	0.02	0.18	0.01	0.16	0.01	0.13	0.05	0.10	0.01	0.13
ε_{yield}	0.16		0.24		0.25		0.17		0.15		0.09		0.21		0.17		0.08	

591

592

593

594

Table 4: Mean absolute percentage error (MAPE) of maximum principal stress between experimentally-derived and optimized material parameters.

	P.1	P.2	P.3	P.4	P.5	P.6	P.7	P.8	P.9
Yeoh	0.7105	0.7398	0.7545	0.4520	0.5303	0.7034	0.2138	0.1754	0.3245
Fung	0.7683	0.1140	0.6022	0.3241	0.7539	0.7130	0.0349	0.2198	0.7034

Figure1

Click here to download high resolution image

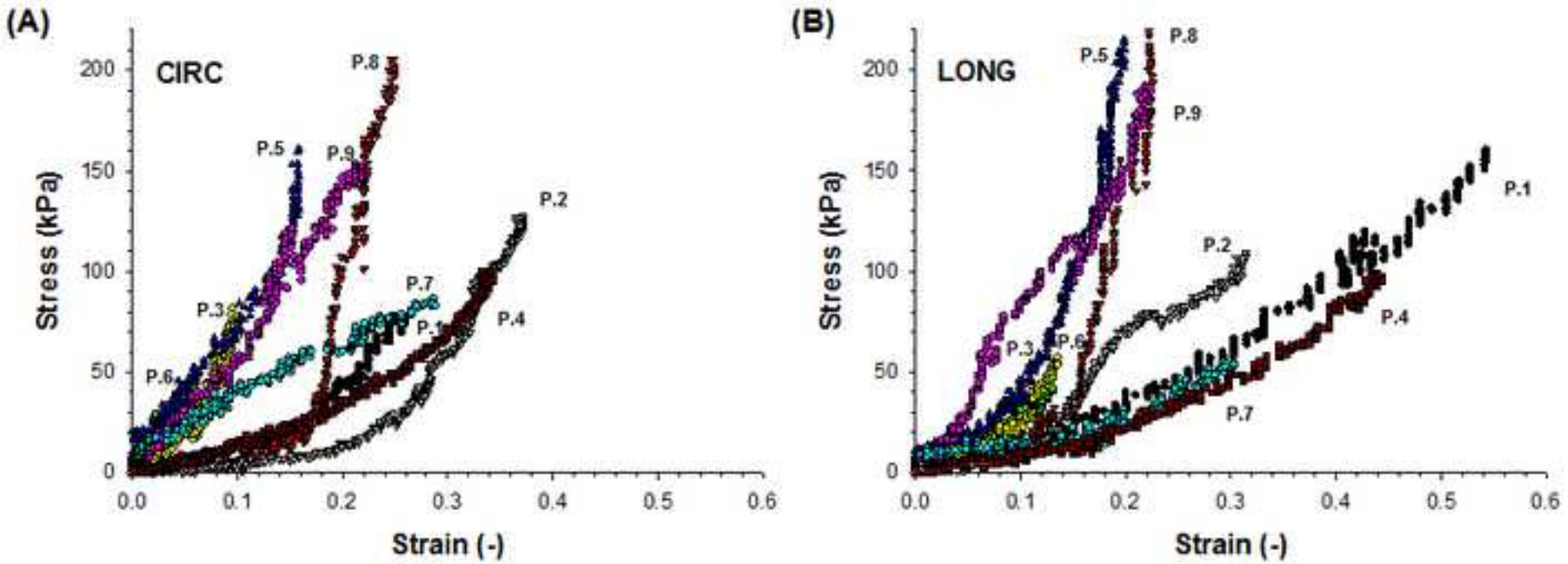

Figure2
Click here to download high resolution image

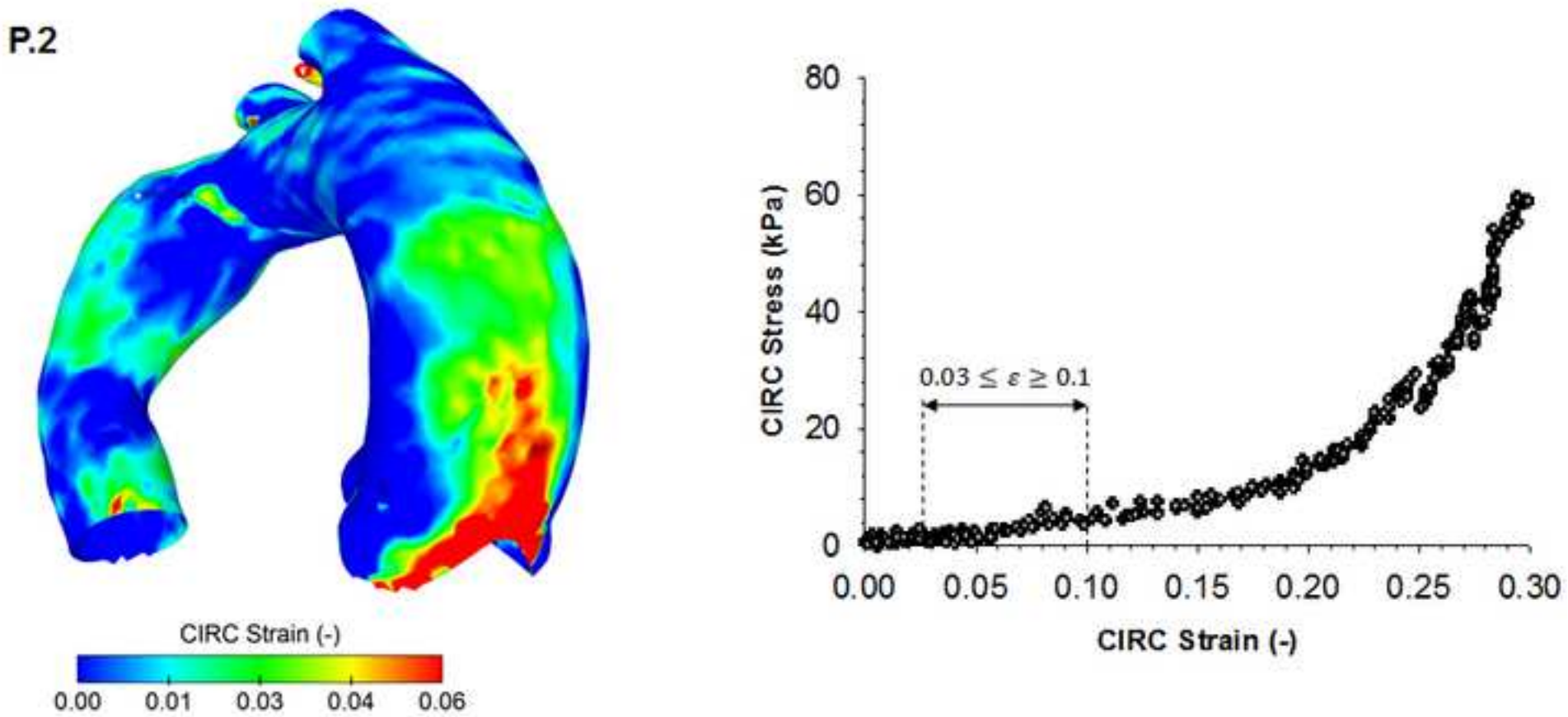

Figure3

Click here to download high resolution image

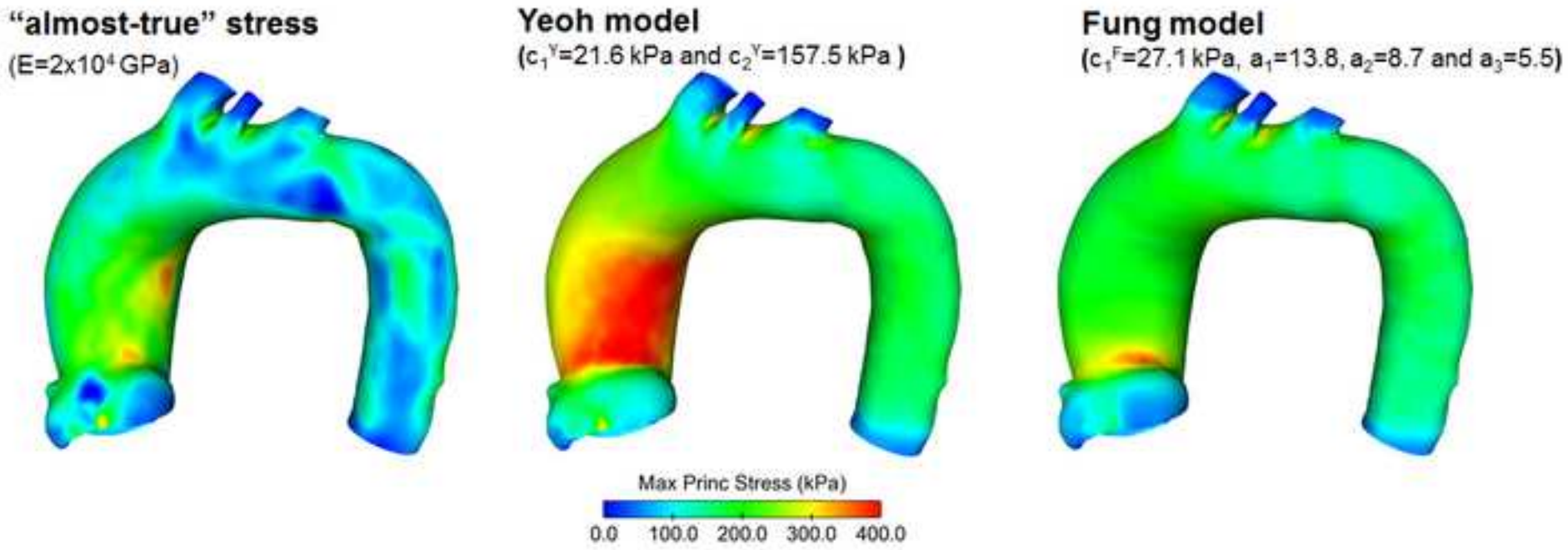

Figure4

Click here to download high resolution image

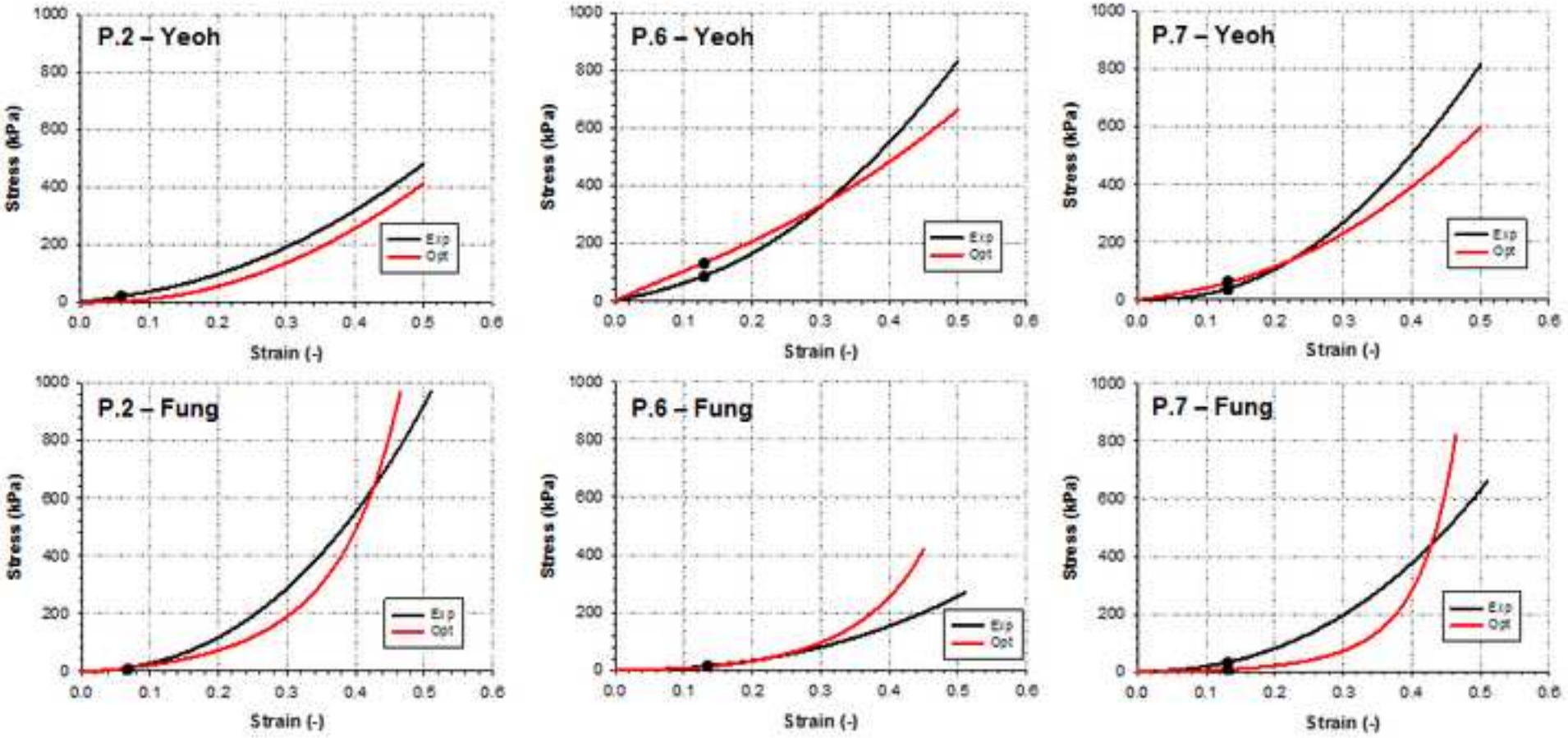

Figure5

Click here to download high resolution image

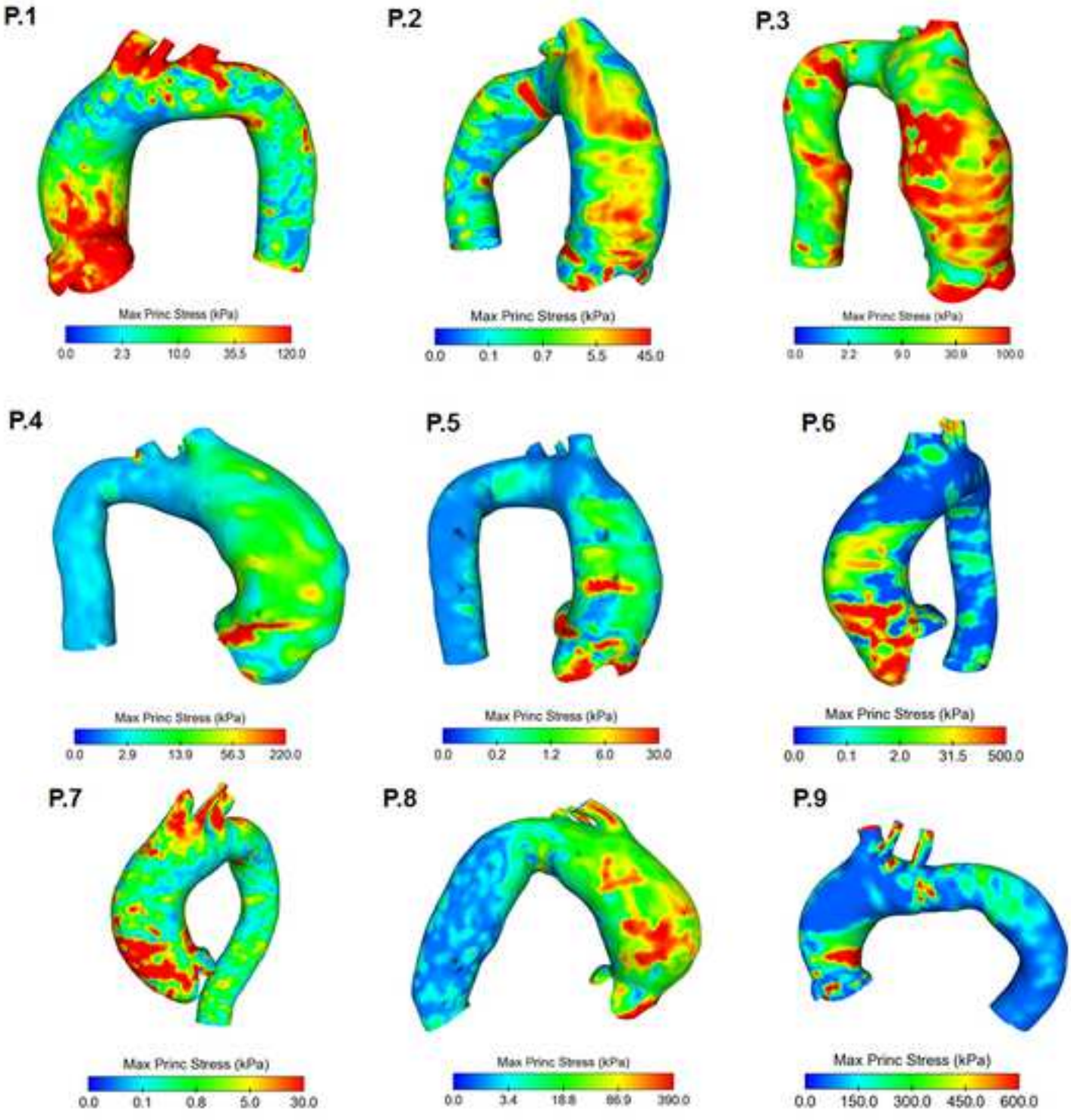

Figure6

Click here to download high resolution image

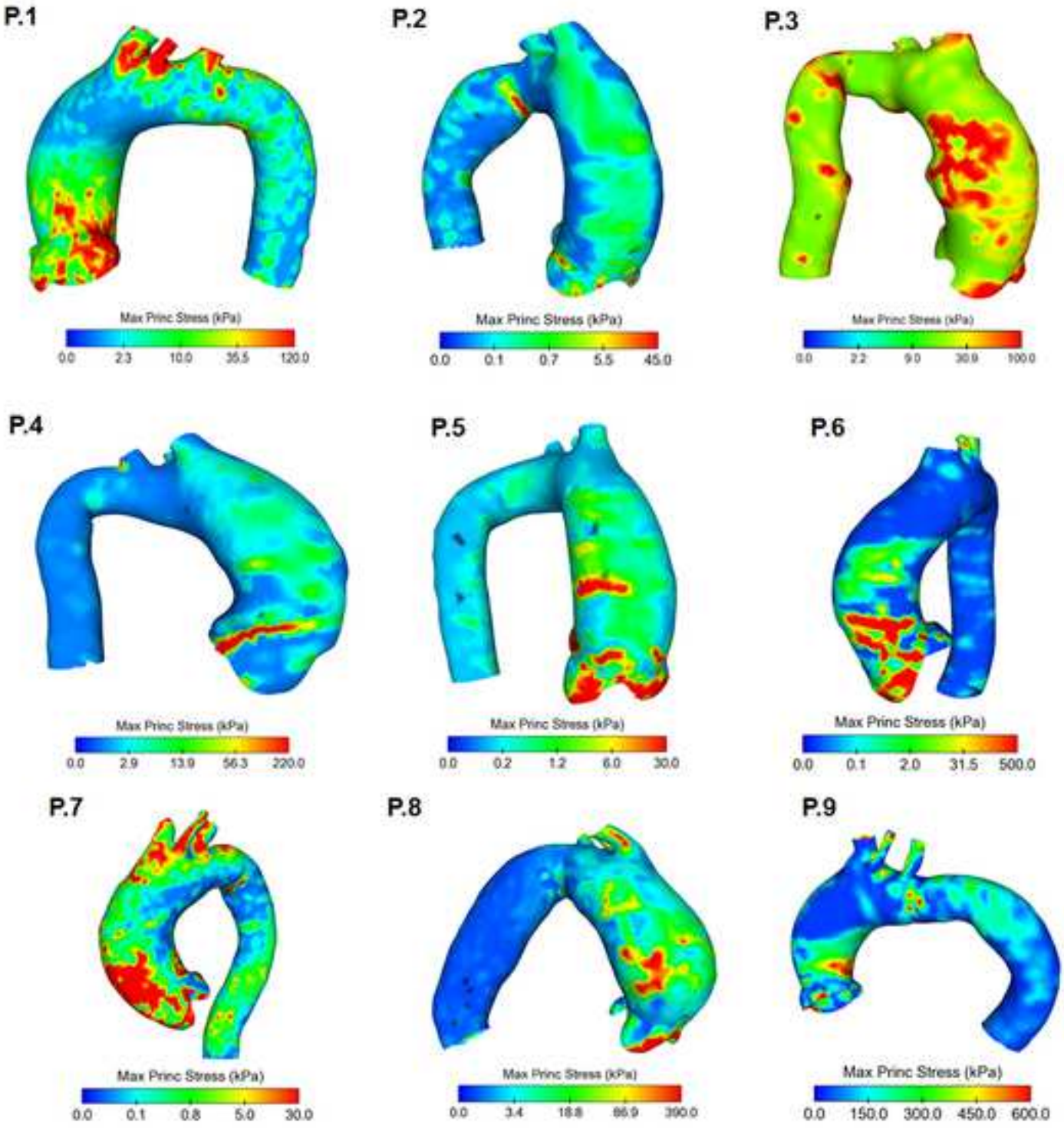

Figure7
Click here to download high resolution image